Marine Geology 496 (2026) 107750

Contents lists available at ScienceDirect

Marine Geology

journal homepage: www.elsevier.com/locate/margo

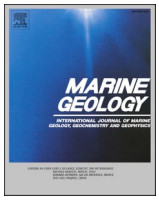

Research Article

A high-resolution record of early rift development and tectonic, sedimentary and environmental conditions in an active rift basin: IODP MSP drilling in the Corinth Rift, Greece (Expedition 381)☆

Lisa C. McNeill [a,1,*], Donna J. Shillington [b,1], Jeanine Ash [c], Gareth D.O. Carter [d], Richard E.Ll. Collier [e], Aleksandra Cvetkoska [f], Paula Diz [g], Mai-Linh Doan [h], Jeremy D. Everest [d], Natacha Fabregas [i], Eugenia Fatourou [j], Mary Ford [k], Robert L. Gawthorpe [i], Gino De Gelder [h], Maria Geraga [l], Jack Gillespie [m], Sophie Green [d,3], Romain Hemelsdaël [n], Emilio Herrero-Bervera [o], Mohammad Ismaiel [p], Liliane Janikian [q], Cari Johnson [r], Aikaterini Kafetzidou [j], Olga Koukousioura [s,t], Katerina Kouli [j], Erwan Le Ber [u,al], Shunli Li [v], Marco Maffione [w], Carol Mahoney [x], Malka L. Machlus [y,z], Fabienne Marret [aa], Ilaria Mazzini [ab], Georgios Michas [ac], Clint Miller [c,2], Casey W. Nixon [i,ad], Sabire Asli Oflaz [ae], Abah P. Omale [af,ag], Konstantinos Panagiotopoulos [j,s], Roberta Parisi [ac], Sofia Pechlivanidou [i,t], Marcie Purkey Phillips [ah], Simone Sauer [ai], Joana Seguin [aj], Spyros Sergiou [l], Natalia V. Zakharova [ak]

[a] School of Ocean and Earth Science, University of Southampton, Southampton, United Kingdom
[b] School of Earth and Sustainability, Northern Arizona University, Flagstaff, AZ, USA
[c] Department of Earth, Environmental and Planetary Sciences, Rice University, USA
[d] British Geological Survey, The Lyell Centre, United Kingdom
[e] School of Earth, Environment and Sustainability, The University of Leeds, United Kingdom
[f] Department of Animal Ecology and Systematics, Justus Liebig University, Germany
[g] Centro de Investigación Mariña, XM1, Universidade de Vigo, Vigo 36310, Spain
[h] Université Grenoble Alpes, Université Savoie Mont Blanc, CNRS, IRD, Université Gustave Eiffel, ISTerre, 38000 Grenoble, France
[i] Department of Earth Science, University of Bergen, Bergen, Norway
[j] Department of Geology and Geoenvironment, National and Kapodistrian University of Athens, Greece
[k] CRPG, UMR 7358, Université de Lorraine, ENSG, INP, France
[l] Department of Geology, University of Patras, Greece
[m] Institute of Earth Sciences, Faculty of Geosciences and Environment, University of Lausanne, Lausanne CH-1015, Switzerland
[n] GeoRessources, University of Lorraine, France
[o] University of Hawai'i at Manoa, Hawai'i Institute of Geophysics and Planetology, USA
[p] Indian Institute of Science Education and Research-Pune, Department of Earth and Climate Science, Maharashtra, India
[q] Instituto do Mar, Universidade Federal de São Paulo, Brazil
[r] Department of Geology and Geophysics, University of Utah, Salt Lake City, UT, USA
[s] Institute of Geology and Mineralogy, University of Cologne, Cologne, Germany
[t] School of Geology, Aristotle University of Thessaloniki, Thessaloniki, Greece
[u] Géosciences Montpellier, Université de Montpellier, France
[v] School of Energy Resources, China University of Geosciences, Beijing, China
[w] School of Geography, Earth and Environmental Sciences, University of Birmingham, United Kingdom
[x] Department of Geography, Northumbria University, Newcastle-upon-Tyne, United Kingdom
[y] Lamont-Doherty Earth Observatory of Columbia University, Palisades, NY, USA
[z] Department of Physical Sciences, Kingsborough Community College, City University of New York, USA
[aa] School of Environmental Sciences, University of Liverpool, Liverpool, United Kingdom
[ab] CNR, Istituto di Geologia Ambientale e Geoingegneria, Area della Ricerca di Roma 1, via Salaria km 29,300, 00015 Montelibretti, RM, Italy
[ac] Institute of Geodynamics, National Observatory of Athens, Athens, Greece
[ad] Equinor ASA, Sandsliveien 90, 5254 Bergen, Norway
[ae] Graduate School "Human Development in Landscapes", Christian-Albrechts-Universität zu Kiel, Germany

☆ This article is part of a Special issue entitled: 'MSP ocean drilling' published in Marine Geology.

* Corresponding author.
E-mail address: lcmn@soton.ac.uk (L.C. McNeill).

https://doi.org/10.1016/j.margeo.2026.107750
Received 30 April 2025; Received in revised form 4 March 2026; Accepted 13 March 2026
Available online 16 March 2026

[af] Department of Geology and Geophysics, Louisiana State University, USA
[ag] BP America, 501 Westlake Park Boulevard, Houston, TX 77079, USA
[ah] Institute for Geophysics, University of Texas at Austin, USA
[ai] Ifremer, Department of Marine Geosciences, Centre Bretagne, France
[aj] Leibniz University Hannover, Institute of Earth System Sciences, Physical Geography and Landscape Ecology Section, Schneiderberg 50, 30167 Hannover, Germany
[ak] Department of Earth and Atmospheric Sciences, Central Michigan University, USA
[al] School of Geography, Geology and the Environment, University of Leicester, United Kingdom

ARTICLE INFO

Editor: Michele Rebesco

Keywords:
Continental rifting
Normal faulting
Basin development
Sedimentary processes
Climate-tectonic-sedimentation interactions
Paleoclimate and paleoenvironment
IODP Expedition 381
Gulf of Corinth

ABSTRACT

The Corinth Rift in Greece is very active, with high rates of extension, sedimentation and environmental change. International Ocean Discovery Program (IODP) Expedition 381 drilled three sites sampling *syn*-rift sediments, complementing previous fault and stratigraphic interpretations and providing the longest high-resolution stratigraphic record for an early phase rift. Sedimentation in the Gulf of Corinth started ~2.0–2.5 Ma as an isolated basin, with the most recent rift phase starting at ~0.75 Ma, marking a shift to increasingly orbitally-controlled marine incursions. A wide range of paleoenvironmental conditions have been generated, reflected in the diverse microfossil assemblages and sedimentary lithologies. Drilling results highlight a recent acceleration of strain rate and fault activity connected to rapid strain localization, with linkage of the border fault system over 10s–100s kyr timescales. Over long timescales (100s kyr), these variations in fault slip rate control sediment accumulation. On shorter time scales (10s kyr), changes in accumulation rate and type of sediment are primarily controlled by glacial-interglacial climate change, with accumulation rates in glacial periods at least double that of interglacial periods, accompanied by enhanced basin stratification and dominance of non-marine faunal assemblages. The mud-dominated sediments have three stratal package types (bioturbated, bedded, laminated) that record distinct hydrological conditions linked to climate and sea level which influence the landscape and basin conditions. Results from the Corinth Rift are compared with other active basins and rift systems for a better understanding of the tectonic and climatic processes shaping these environments.

1. Introduction

This paper constitutes an overview of the objectives and synthesis of the achievements so far from IODP Expedition 381 in the Corinth Rift, one of the Mission Specific Platform expeditions of IODP, as part of a Special Issue volume entitled “Twenty years of Mission Specific Platform expeditions in scientific ocean drilling”.

1.1. Rift Evolution

Continental rifting is the first stage of the process that can lead to continental breakup and ocean basin formation. However, the style and variability of deformation in the first few Myr of this process are often less well known due to deep burial and overprinting within more mature passive margins or failed rift systems and the relatively small number of active rift systems worldwide. The magnitude, rate and timing of deformation during this early stage of rifting have rarely been quantified at high temporal resolution (10s - 100 s kyr). For many studies, the finest achievable rift-scale temporal resolution is of the order of ≥1 Myr, such that the details of the rift evolution process are missed. Results from this study show that significant changes in rift structure and rate of process occur on timescales <1 Myr.

Over the last ~15–20 years, important insights have been derived from numerical models (e.g., Olive et al., 2014; Naliboff et al., 2017; Pan et al., 2022; reviews of Pérez-Gussinyé et al., 2023 and Zwaan et al., 2024) and from observations at mature, magma-poor passive margins, including on the Newfoundland margin (e.g., Van Avendonk et al., 2009) and the Galicia margin (e.g., Bayrakci et al., 2016) where activity has ceased. The results demonstrate that different modes of extension of the crust are possible, and that these likely combine and vary in space and time (e.g., Peron-Pinvidic and Manatschal, 2019). In addition, high-resolution geophysics and borehole drilling in active continental rifts have provided constraints on temporal changes in fault activity and basin evolution (e.g., Muirhead et al., 2019; Scholz et al., 2020). Many previous studies have noted localization of strain within a rift, often towards the rift axis (e.g., Cowie et al., 2005, 2007), although others show increased distribution of strain with time (e.g., Bell et al., 2014). But details of the timing relative to the onset of rifting and the rate of localization and its variability along a rift are not always resolved, nor at high resolution. Both models and observed rift examples tend to show a primary rift border fault system developing and taking up much of the extensional strain as part of this localization process (e.g., Walsh et al., 2003; Scholz et al., 2020), but how and when this fault system becomes established relative to onset of rifting is not always established.

The Corinth Rift, the subject of this paper, is a focused site of rifting within the wider Aegean rift system. Its scale (~150 km in length, ~50 km in width) is comparable to other active rift systems (e.g., in the East Africa Rift) but smaller than the largest extensional domains (e.g., the Basin and Range). Mature rifted margin systems can extend for 100's to 1000 km's in length (e.g., Atlantic rifted margins). Likewise, fault length exhibits a continuum of scales in both active and inactive rift systems (Lathrop et al., 2022). Individual border faults in active rift systems can be 10's km - >100 km in length (e.g., Ebinger and Scholz, 2012; Shillington et al., 2020; Nixon et al., 2016), but several can link, forming structures potentially several 100 km's in length. These structures are comparable in scale to major fault structures on mature rifted margins (e.g., Lei et al., 2020; Muñoz-Barrera et al., 2021). The Corinth Rift itself has individual border faults of 10–20 km length linked to form an ~100 km structure. Despite variability in spatial and temporal scales between rifts, the new results on rift evolution in the Gulf of Corinth capture basic processes common to many rifts worldwide, such as normal fault growth and linkage. Given that major structures formed early in the rift process may influence rifted margin structure (e.g., Naliboff et al., 2017), the results presented here are relevant to global studies of rift systems at different stages of evolution.

1.2. Rift paleoenvironment and sedimentation

As a continental rift evolves, it transitions from a terrestrial environment above mean sea level to lacustrine/isolated rift basins (above or at sea level) and finally to connection with an ocean basin. This

[1] These authors contributed equally to this work
[2] Present address: J.S. Held LLC, Jericho, NY, USA
[3] Present address: Zero Waste Scotland, Stirling, UK

progression is largely driven by lithospheric thinning and tectonic subsidence. In detail, this relates to how the rate of tectonic subsidence changes over time as the crust and lithosphere extend and thin, which in turn is related to rift faults growing, dying, and linking. On shorter time scales, paleoenvironment is primarily controlled by climate that drives sea level fluctuations and evaporation-precipitation patterns and rate of sediment flux filling the basin. For continental rifts, our understanding of these processes and the resulting basin paleoenvironment and patterns of sedimentation has been based on models (e.g., Gawthorpe and Leeder, 2000) and on a small number of ground-truthed active rifts or exposed earlier stratigraphic sequences (e.g., Gawthorpe et al., 1990; Dorsey and Umhoefer, 2000; Lyons et al., 2015). Overall, few active rifts are going through this process today or details are deeply buried in now inactive rifted margins or failed rifts where the level of temporal and spatial detail is limited. In addition, deep sampling (drilling) in active rift systems is quite rare. An exception is drilling in the Lake Malawi (Nyasa) Rift (e.g., Lyons et al., 2015). Here lake level variations of 200–400 m are recorded, impacting the basin environment; however, this rift is not yet at the stage of ocean connection, thus lacks constraints on this important environmental transition. Tectonically-controlled basins at the stage of periodic connection to the open ocean (fluctuating between lake and sea conditions as sea level changes or basin sills move vertically) have been studied previously, e.g., the Black Sea and the Sea of Marmara. Here basin paleoenvironmental change can be linked to climate and sea level but the present tectonic setting at these locations is not an active rift. In the case of the Black Sea, drilling has sampled a long sedimentary record of changing environment (Hsü, 1978) but this has relatively low resolution and is in an environment of lower tectonic activity albeit with large amplitude of sea level change (e.g., Aksu and Hiscott, 2022).

Although it has been long understood that climate and tectonics interact to control sediment input to a rift basin and the environment of that rift basin as rifting progresses (e.g., Gawthorpe and Leeder, 2000; Dorsey and Umhoefer, 2000), it is rarely established in what circumstances tectonics versus climate dominates these environmental processes or on what timescales, because there are few or no studies with a 10-kyr resolution of the *syn*-rift sedimentation pattern. In this paper we aim to address the questions raised on Rift Evolution above and on Rift Paleoenvironment and Sedimentation using the new high-resolution temporal and spatial record from the Corinth Rift.

1.3. The Corinth Rift

The Corinth Rift (Fig. 1) has exceptionally high rates of active extension (extension rates are up to 10–20 mm/yr; Avallone et al., 2004). These high rates of activity (and hence resolution), alongside its youth (<5 Myr) and hence clarity of its geological record, make Corinth a natural laboratory for evaluating early rift evolution, and for comparison to observations and models of rifts that evolve to oceans (e.g., Bell et al., 2009; Nixon et al., 2024). The Corinth Rift is compact (~150 × 50 km) and a closed, small-scale clastic sedimentary system. The last ~2 Myr of the *syn*-rift stratigraphic record is preserved offshore while earlier rift sediments are preserved onshore, providing a clear spatial and temporal record of rift activity. The offshore rift has been surveyed creating a dense network of seismic reflection data (line spacing of ~1–5 km; e.g., Fig. 2; Nixon et al., 2016) that provide high-resolution spatial information on the distribution of syn-rift sediments and the fault network (e.g., Sachpazi et al., 2003; Taylor et al., 2011).

Corinth rifting began ~4 Ma with three main phases identified by integrating onshore deposits and offshore seismic stratigraphy (e.g., Sachpazi et al., 2003; Nixon et al., 2016; Ford et al., 2017; Gawthorpe et al., 2018). As the rift has developed over these three phases (e.g., Ford et al., 2017), it has both migrated north (likely linked to the rollback of the underlying subducting African plate) and varied in width. In the Gulf of Corinth, the grid of seismic reflection data has been used to resolve spatial patterns of fault and depocenter development and estimate timings and rates - e.g., the geometry of dominant faults and of the rift basin itself (Fig. 1), linkage history of faults, the merging of depocenters over time, and fault slip rates (e.g., Bell et al., 2009; Taylor et al., 2011; Nixon et al., 2016). Key results from these studies include that: (i) patterns of extension change along the rift axis and with time, with strain distributed across multiple active faults in the west but focused on 1–2 primary faults in the centre and east; (ii) the rift geometry has changed from a more symmetrical pattern of both N- and S-dipping faults to predominantly N-dipping faults and hence towards basin asymmetry; (iii) slip rates of the major faults are high and estimated as up to 5–10

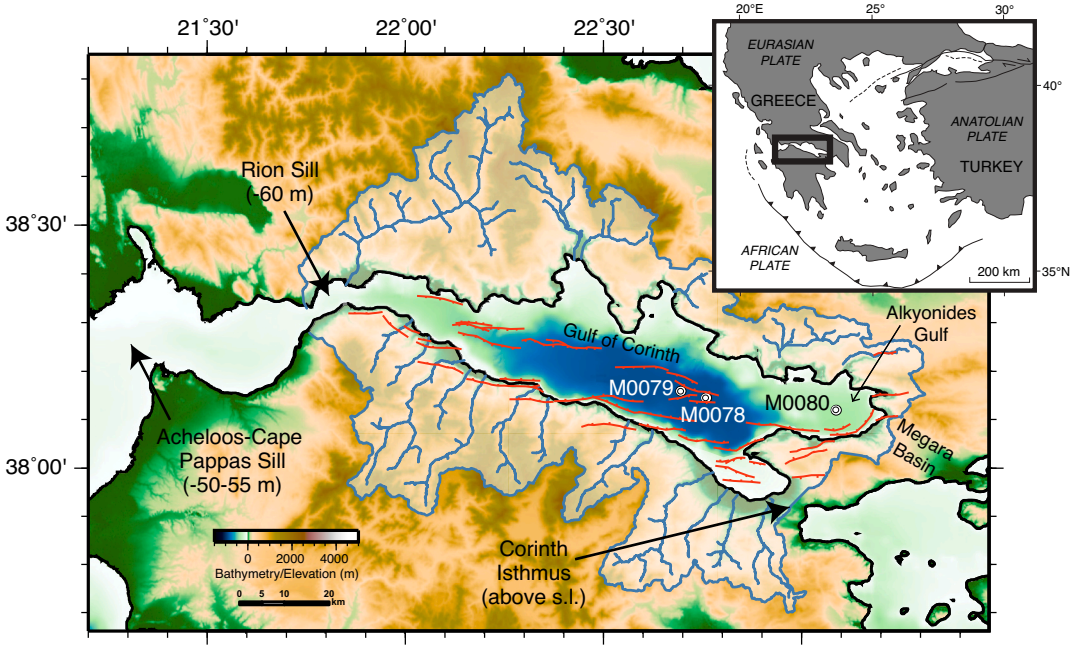

Fig. 1. Map of Gulf of Corinth and Corinth Rift including major active faults, IODP Expedition 381 drill sites, basin-bounding sills and their approximate depths today (an additional sill sits south-east of the Corinth Isthmus in the Saronic Gulf, outside the figure area), and catchment areas (from McNeill et al., 2019b). Inset shows tectonic setting within the Eastern Mediterranean region.

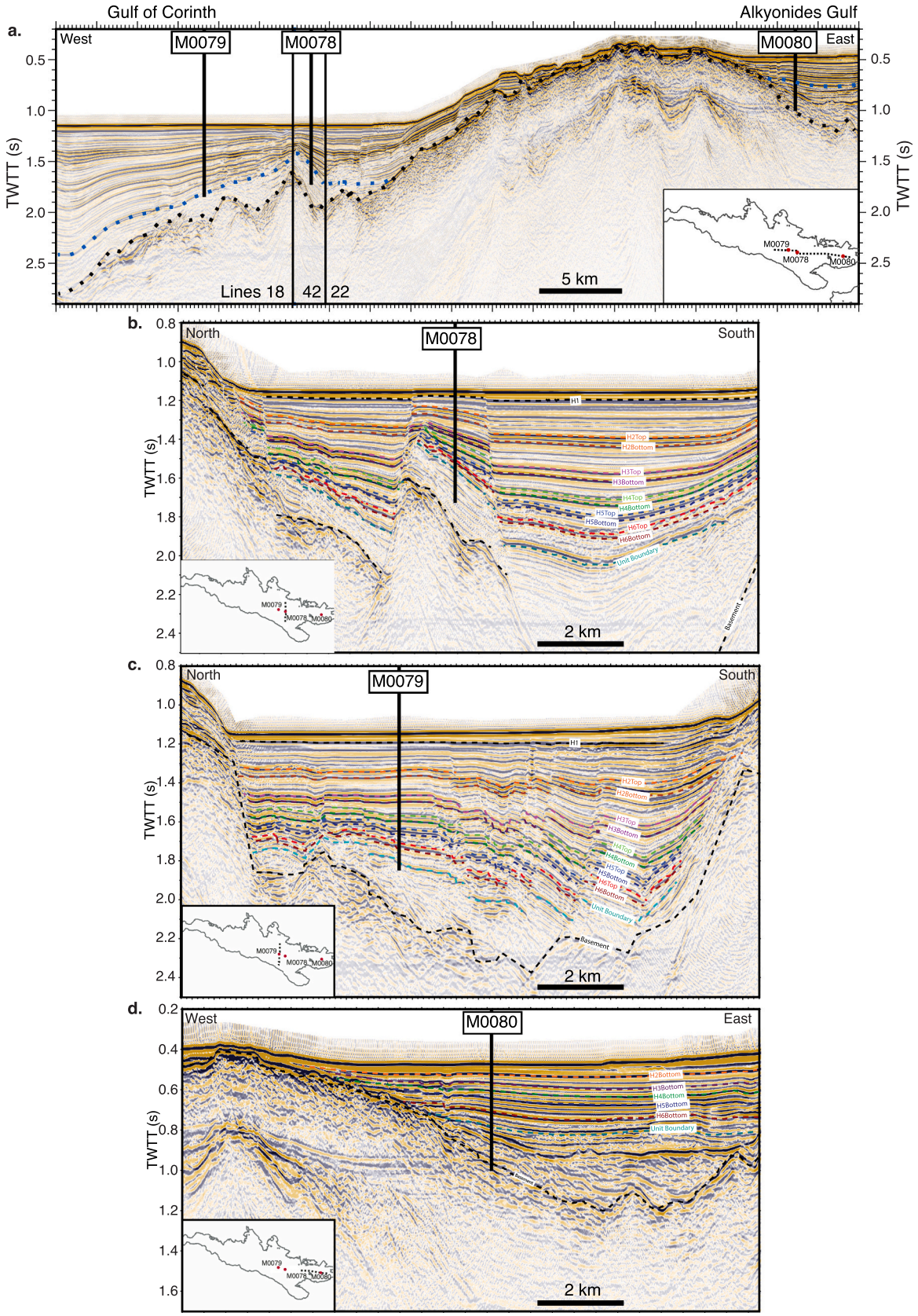

Fig. 2. Seismic reflection profiles with IODP site locations. a) Composite profile along rift axis connecting the three drill sites. b), c) and d) Profiles across each drill site. Seismic profiles are from Taylor et al. (2011), seismic interpretation from Nixon et al. (2016, 2024).

mm/yr; and (iv) the *syn*-rift fill initiated in two separate depocenters that later merged into a single depocenter as the rift matured (e.g., Bell et al., 2009; Nixon et al., 2016).

During the first phase of rifting (estimated timing ~4–2 Ma depending on the position along the rift axis), the onshore exposures suggest a terrestrial environment from alluvial to deep lacustrine sediments (e.g., Ford et al., 2013; Gawthorpe et al., 2018; Hemelsdaël et al., 2021). The second phase of rifting (estimated timing prior to drilling results: ~2.5–1.8 Ma to ~0.7–0.45 Ma; e.g., Nixon et al., 2016) was shifted to the north and involved development of large fan delta systems feeding into a basin of likely lacustrine/isolated environment. Some of the sediments from this rift phase are uplifted and exposed onshore and others are preserved offshore within the Gulf of Corinth. The third phase of rifting (estimated timing prior to drilling results: ~0.7–0.45 Ma to present) is characterized by alternating marine and isolated environments and deposition, interpreted from shallow sediment cores and seismic stratigraphic character (e.g., Perissoratis et al., 2000; Sachpazi et al., 2003; Lykousis et al., 2007) and controlled by sills surrounding the basin and eustatic sea level fluctuations. Such alternations in paleoenvironment were proposed by many studies from seismic data before drilling (e.g., Lykousis et al., 2007; Bell et al., 2009; Nixon et al., 2016), and the most recent transition from isolated to marine ~12 ka was identified in shallow piston cores (Collier et al., 2000; Perissoratis et al., 2000; Moretti et al., 2004). The deposits preserved in the Gulf of Corinth (drilled in IODP Expedition 381) represent the most recent two phases of rifting and reach a thickness of up to 2.5 km.

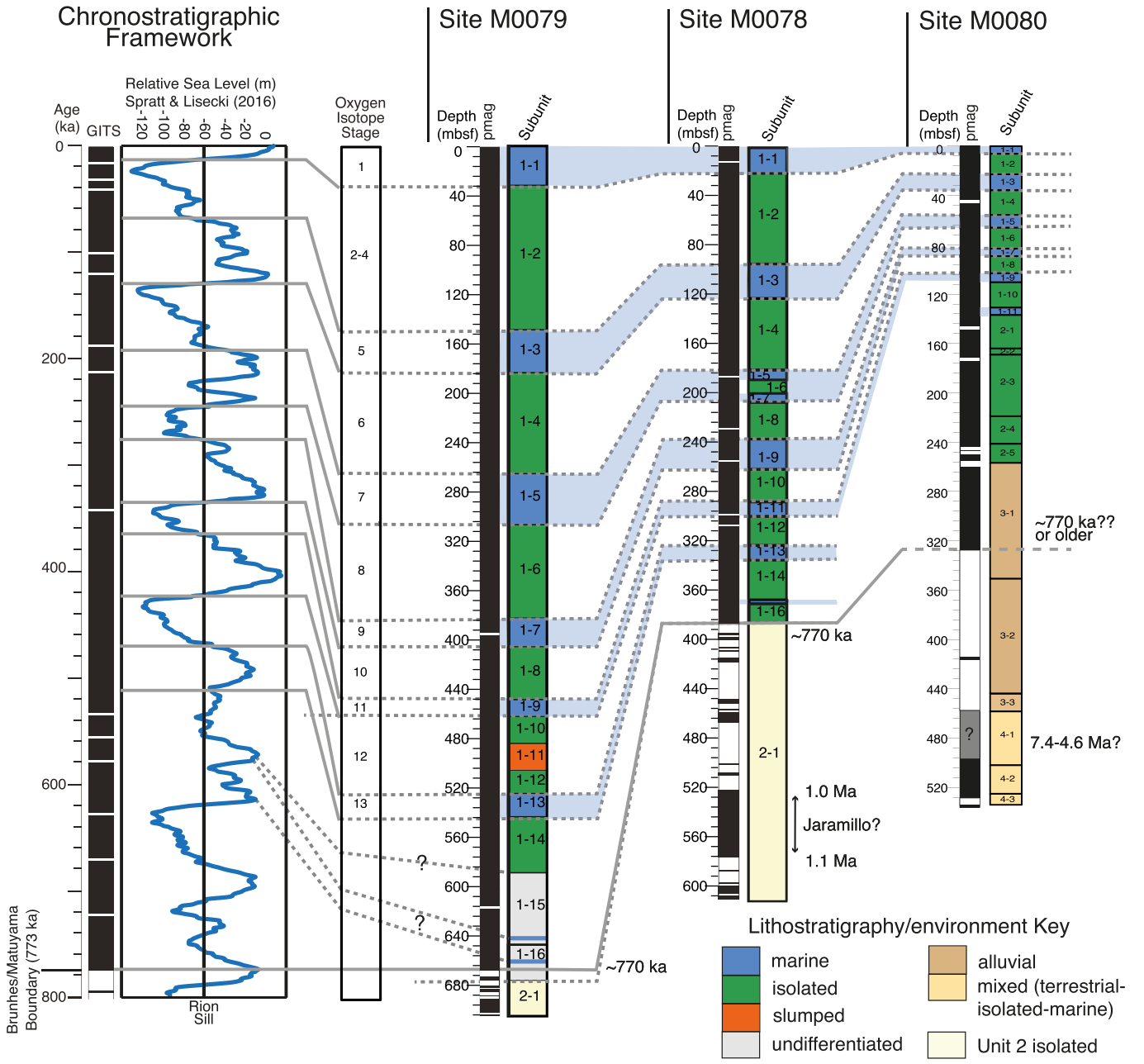

Fig. 3. Lithostratigraphic units and paleomagnetic data for each of the three drill sites, correlated to the eustatic sea level curve (Spratt and Lisiecki, 2016) and oxygen isotope stages (see also McNeill et al., 2019a, 2019b). See Syn-rift Chronology section for information on dating techniques used to construct this correlation. Dates shown are primary magnetostratigraphic markers (Brunhes-Matuyama chron boundary at 773 ka; potential Jaramillo subchron at 1–1.1 Ma; Maffione and Herrero-Bervera, 2022; McNeill et al., 2019a) and earlier age control in Site M0080 (calcareous nannofossil ages and U/Pb dates on calcareous siltstones; Hemelsdaël et al., 2024; M. Purkey Phillips, pers. comm., 2025). mbsf=meters below seafloor.

2. IODP Expedition 381

IODP Expedition 381 acquired 1645 m of recovered core over 1905 m of cored intervals at three sites, two in the Central Gulf of Corinth and one in the Alkyonides Gulf (Fig. 1). The offshore component of this Mission Specific Platform expedition occurred aboard the D/V *Fugro Synergy* in October–December 2017, and the onshore science party took place at the MARUM and University of Bremen, Germany in February 2018. The objectives of IODP Expedition 381 were to constrain the temporal and spatial evolution of faulting and surface processes in a young rift, improve regional hazard assessments, and reconstruct paleoclimate and paleoenvironment in the Gulf of Corinth and eastern Mediterranean Sea. The cores obtained by IODP Expedition 381 address these objectives by providing (1) a long history of rifting, sedimentation, and paleoenvironment (sites M0078 and M0080), (2) a high-resolution record of processes in the last ~800 kyr (Site M0079), and (3) the spatial variation of rift evolution (comparison of sites in the central versus eastern rift) (Fig. 1). Below we review and synthesize highlights of current results from this expedition.

3. Syn-rift Chronology from Drilling and Stratigraphic Correlation

One of the primary purposes of drilling was to establish a chronology for the *syn*-rift sediments sampled, enabling the history of rift evolution and rates of process to be established with confidence; in previous chronologies, timings and rates were only estimated or ground truthed by sampling as far back as ~50 ka (e.g., Nixon et al., 2016). Multiple dating techniques were used during the expedition, and these have been supplemented with additional analyses since the expedition. Detailed results of these techniques can be found in the IODP 381 Expedition Report (McNeill et al., 2019a) and in several published studies (McNeill et al., 2019b; Gawthorpe et al., 2022; Maffione and Herrero-Bervera, 2022; Mazzini et al., 2023; Hemelsdaël et al., 2024; Nixon et al., 2024; Sergiou et al., 2024; Pechlivanidou et al., 2025). The chronology at each site has been used to make a stratigraphic correlation between the three boreholes (Fig. 3).

Techniques used for dating include:

a) Cyclical paleoenvironment and links to the eustatic sea level curve.

The drill cores confirmed that the basin environment fluctuated between marine and isolated conditions within the most recent rifting phase or upper unit (Unit 1; Fig. 3), primarily on the basis of the microfaunal and microfloral assemblages present (McNeill et al., 2019a, 2019b; Gawthorpe et al., 2022; Fatourou et al., 2023, 2025; Mazzini et al., 2023; Nixon et al., 2024; Parisi et al., 2024). Sub-units within each borehole were established from these changes through time (Fig. 3), and these also correspond to sedimentary facies and lithology changes (Gawthorpe et al., 2022; Fig. 4) and physical properties changes of the sediments (McNeill et al., 2019a). Using the present-day basin sill depth (Rion sill ~50–60 m; McNeill et al., 2019b; Fig. 1), a date was assigned to each subunit boundary based on the eustatic sea level curve of Spratt and Lisiecki (2016) (Fig. 3). In Unit 2 (the penultimate rifting phase), the sediments are more homogenous in lithology, lacking the cyclical stratigraphy, and are interpreted as predominantly isolated in environment, therefore the same approach cannot be applied.

b) Biostratigraphy.

Calcareous nannofossil assemblages were interpreted throughout the stratigraphic sequence at each borehole (Fig. 5; McNeill et al., 2019a, 2019b). The Last Occurrence of *Pseudoemiliania lacunosa* and the First Occurrence of *Emiliania huxleyi* were used to place approximate tie points in the upper unit (Unit 1) of the age model. The precise ages of these tie points are complicated in the Corinth record because of the unusual paleoenvironment and discontinuous marine sequence (M. Purkey Phillips, pers. comm., 2025). At Site M0080, rare calcareous nannofossils were observed in the oldest sediments (Unit 4) and are interpreted to be *in situ*. These are assigned an approximate age of Late Miocene to Early Pliocene (Fig. 3), consistent with U/Pb dates on calcareous silts in this unit (Hemelsdaël et al., 2024). This unit, therefore, represents an earlier phase of rifting, likely an extension of the Megara basin in the east of the rift system.

c) Magnetostratigraphy.

Magnetostratigraphic analyses identified the Brunhes-Matuyama chron boundary (0.773 Ma) in all three sites (although tentatively in Site M0080), and the Jaramillo subchron (1.001–1.076 Ma) in Unit 2 of Site M0078 (McNeill et al., 2019a, 2019b; Maffione and Herrero-Bervera, 2022). In addition, a relative paleointensity (RPI)-calibrated age model was developed for Site M0079 (Maffione and Herrero-Bervera, 2022), and further work continues with RPI on the expedition cores.

d) Additional chronological techniques.

During and since the drilling expedition, tephrochronology (McNeill et al., 2019a; Pechlivanidou et al., 2025; unpublished work), radiocarbon dating in the youngest section (e.g., Nixon et al., 2024; Mazzini et al., 2023; Pechlivanidou et al., 2025), U/Th dating of aragonite laminations (Gawthorpe et al., 2022), and U/Pb dating of calcareous silts (Hemelsdaël et al., 2024) have been conducted, and these further refine the age model presented here. These and other dating analyses are ongoing, and the age model will continue to be improved.

Stratigraphic correlation.

Correlation of unit and subunit boundaries was possible between the three sites (Fig. 3). This was most straightforward for the cyclical marine and isolated subunits of Unit 1 (Gawthorpe et al., 2022; Nixon et al., 2024), although not possible for the earliest and thinnest marine intervals in Unit 1 within Site M0080. Here marine environmental intervals were short and marine sediments very thin due to the low sediment accumulation rate in the eastern Alkyonides depocenter (subsiding more slowly due to lower extension rates). Correlations between boreholes in the earlier/deeper parts of the stratigraphy are also more tentative.

4. Rift and fault development

The spatial patterns of rift faulting and depocenter distribution and their relative changes through time were developed prior to drilling, using the offshore grid of seismic reflection data, onshore tectonic geomorphology (from fault-uplifted marine terraces and fault traces) and onshore *syn*-rift stratigraphic exposures (compiled by Nixon et al. (2016) building on other studies, e.g., Bell et al. (2009) and Taylor et al. (2011)). Estimated timings and rates were interpreted by several groups of authors from rare dates onshore and from seismic stratigraphic interpretations offshore (see Introduction). The drilled boreholes now provide a much more robust chronology. Nixon et al. (2024) integrated the existing spatial fault, depocenter and rift element interpretations with the chronology from the new borehole data to develop a detailed analysis of how the rift has developed over the past ~2 Myr (Fig. 6). The main subsequent results and analyses from Nixon et al. (2024) and earlier studies are summarised below.

In the last 2.0–2.5 Myr, the Corinth Rift has experienced a history of rapid changes (on 100 kyr timescales) in active fault position and rift geometry and polarity, even over this short time period which represents the last two phases of rifting and the formation of the Gulf of Corinth. The drilling data have provided rates of fault activity, the timing of changes in depocenter development and fault networks, and subsidence rates over time.

The drilling data provide confirmation of strain localization within the rift and its timing relative to the onset of rifting (Fig. 6). The border fault system (on the southern rift margin; Fig. 1) formed from ~800 ka (Nixon et al., 2024). Linkage of this border fault system between ~500 and 200 ka represents strain localizing on a primary rift fault system (Fig. 6d). The border fault system is interpreted to be kinematically coherently linked from ~130 ka. Coincident with the kinematic linkage

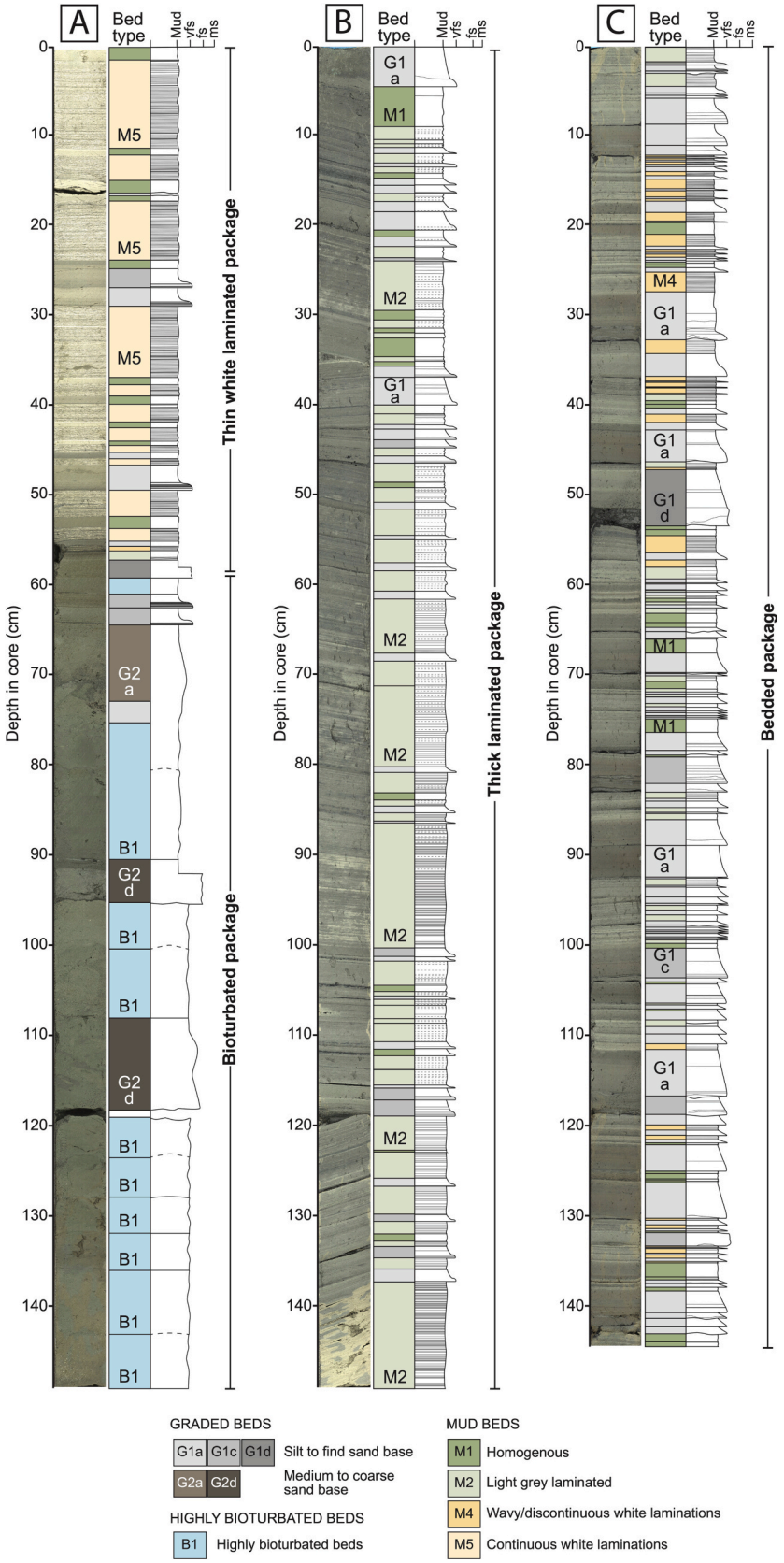

Fig. 4. Examples of stratal packages observed in Lithostratigraphic Unit 1 from sites M0078 and M0079 (from Gawthorpe et al., 2022). Left panels show core images, middle panels show bed classification, and right panels show graphic sedimentary log with grain size. a) Site M0079, Core 45R-2; b) Site M0078, Core 116R-1; c) Site M0079, Core 62R-3. See Gawthorpe et al. (2022) for details. Note dip of bed layers is largely generated by the coring process.

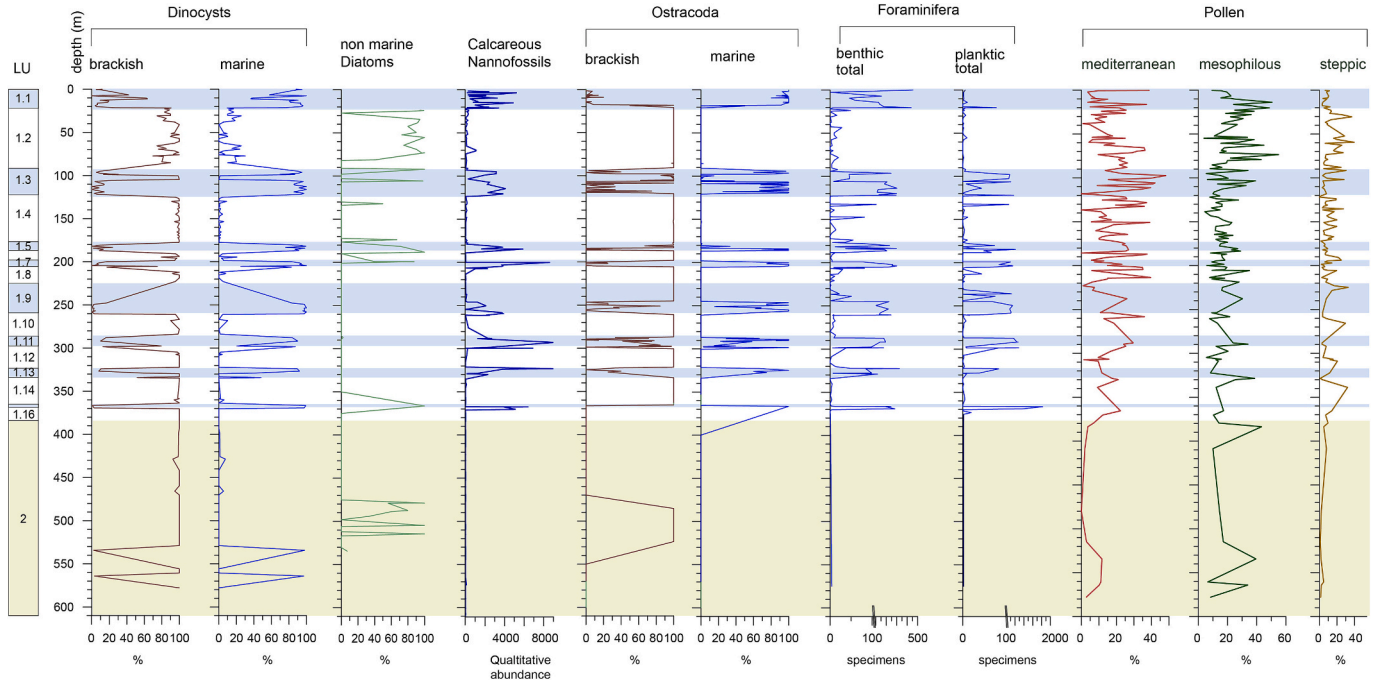

Fig. 5. Summary of microfossil abundances with depth for Site M0078. LU = lithostratigraphic units and subunits. Dinocyst data are from Fatourou et al. (2023) and Fatourou et al. (2025), non-marine diatoms and calcareous nannofossils are from McNeill et al. (2019a), ostracod assemblages are from Parisi et al. (2024) and Parisi et al. (2025), foraminiferal data are from McNeill et al. (2019a), and pollen data are from Kafetzidou et al. (2023). Note that calcareous nannofossils are based on qualitative abundance of species (see McNeill et al., 2019a for details).

of the border fault system and active hanging wall flexure, the activity of S-dipping (antithetic) faults in the border fault hanging wall (part of the set of "intrarift faults") has significantly increased over this recent time period (Nixon et al., 2024).

Extensional strain rates across the rift (based on cumulative fault throw rates, see Fig. 6 in Nixon et al., 2024) have also increased over time as fault linkage and strain localization has occurred, and in particular since 130 ka, as strain has transferred from S-dipping faults to the dominant N-dipping fault systems today (predominantly the border fault system) (Nixon et al., 2016, 2024). This appears to represent a real increase in rift extension through time, rather than an artificial change as a function of incomplete data. Possible explanations for this change are: a) further localization of strain within the Corinth Rift relative to other parts of the wider Aegean extensional province; b) increased extension in the upper crust relative to the lower crust or increased upper-lower crust coupling (e.g., Pérez-Gussinyé et al., 2023), potentially due to the border fault system linking and extending deeper into the crust; c) reaching a threshold of lithospheric thinning and weakening that leads to acceleration of extension (e.g., Brune et al., 2016); or d) an actual increase in relative plate motion in the region. Testing of these scenarios will be the subject of future study.

Fault slip rates for the major active faults are now well constrained based on the new drilling data combined with existing data. These represent some of the highest recorded slip rates of normal faults worldwide, with rates on the border fault system segments over the last 130 kyr of up to 5–8 mm/yr (Nixon et al., 2024). Low-angle extensional detachments can have higher slip rates (e.g., the Mai'iu fault, Woodlark Basin Rift; Webber et al., 2018), but otherwise only faults in the high extension rate Afar rift, Ethiopia appear to come close to Corinth fault rates (e.g., 3.8–5 mm/yr on the western Danakil depression margin; Bastow et al., 2018). The high fault slip rates confirm the significant earthquake hazard potential of the Corinth Rift. Nixon et al. (2024) compared fault slip rates with seismic moment release from historic and instrumented earthquakes and identified seismic deficit (or gap) in the central and western rift.

The drill cores also provided the opportunity to investigate potential evidence (or absence of evidence) for earthquakes in the sedimentary record. De Gelder et al. (2021) made a detailed analysis of turbidite-homogenite packages that may represent earthquake-triggered gravity flows in the basin. They found complex but characteristic sedimentary features of the larger (>10 cm thick) of these deposits that may result from earthquake shaking, however results should be interpreted cautiously as multiple triggers and processes, beyond earthquakes, can be involved in generating sediment gravity flows (Gawthorpe et al., 2022). Interestingly, there is a general lack of debrites, matrix-supported conglomerates and slumped beds within the drill cores (interpreted as deposits from debris flows and transitional flows; Gawthorpe et al., 2022; see also Figs. 3 and 4 and "Controls on flux, lithology, and distribution of sediments" section below). This suggests that either this type of slope instability event (be it triggered by earthquakes, storms or other processes) is relatively rare, or that this type of flow does not reach the central basin position of the drill sites.

5. A new record of Mediterranean paleoenvironment and paleoclimate

The Expedition 381 cores provide the first observations of variations in paleoenvironment within the Corinth Basin over the last ~5 Myr and add new offshore constraints to the onshore record of variations in Mediterranean paleoclimate (e.g., Follieri et al., 1989; Tzedakis et al., 1997, 2006; Sánchez Goñi et al., 1999; Reille et al., 2000; Donders et al., 2021). Corinth is one of the only regions where it is possible to combine the terrestrial vegetation record with the marine environmental record (Fatourou et al., 2023, 2025; Kafetzidou et al., 2023). Many studies are ongoing with this combined dataset, but here we highlight a few examples from published work.

Cores from all three drill sites document alternating paleoenvironments in the rift as sea level fluctuated with respect to sills at the edges of the Gulf of Corinth over the last ~780 kyr, with marine conditions during interglacials and isolated conditions during glacials in the

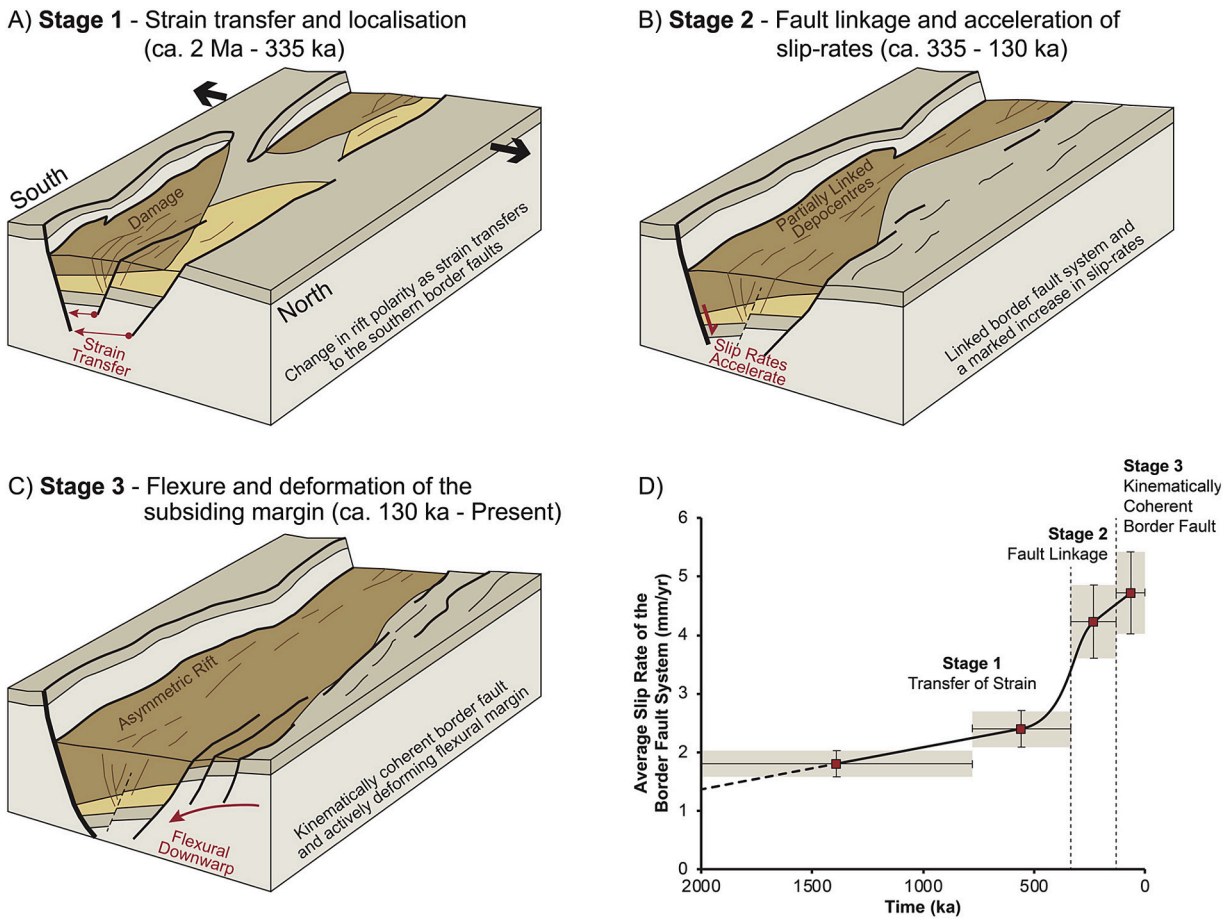

Fig. 6. A-C: Cartoons of stages of rift development from ~2 Ma to present. D: average slip rate of the now dominant border fault system over time (from Nixon et al., 2024).

Central Gulf (Figs. 3, 5). Site M0080 also records these fluctuations, but the Alkyonides Gulf environment may differ, being separated from the Gulf of Corinth by another sill. Although alternations in paleoenvironment have been previously proposed (see Introduction), Expedition 381 was the first documentation of these variations over hundreds of thousands of years and over multiple oxygen isotope and sea level cycles (McNeill et al., 2019b).

Changing paleoenvironment within the basin is reflected in microfossil assemblage changes in the Expedition 381 cores (Fig. 5). The assemblages provide a detailed record of the alternating conditions within the basin, with substantial shifts between marine and brackish assemblages (e.g., Fatourou et al., 2023, 2025; Parisi et al., 2025). Benthic and planktic foraminifers, ostracods, nannofossils, marine dinoflagellate cysts and diatoms are very abundant in interglacial intervals (Fig. 5) indicating the establishment of fully marine conditions in the basin. In contrast, during the glacial intervals, the basin was dominated by brackish dinocysts, ostracods and non-marine diatoms (McNeill et al., 2019a, 2019b; Gawthorpe et al., 2022; Fatourou et al., 2023; Mazzini et al., 2023; Parisi et al., 2024). Dinocysts (Fatourou et al., 2023, 2025), ostracods (Mazzini et al., 2023) and rare marine diatoms and nannofossils within isolated glacial subunits specifically indicate brackish and not freshwater conditions at these times. Furthermore, the brackish species of the ostracod and dinocyst assemblages have clear similarities to those of the early Holocene in the Black Sea and those presently found in the Caspian Sea (e.g., Marret et al., 2009; Mudie et al., 2017), and these aid interpretations of water mass exchanges between water bodies in the region.

Pollen analyses of the Expedition 381 cores were used to interpret changes in vegetation composition and cover in the borderlands surrounding the Gulf of Corinth over time (Fig. 5), allowing a correlation of the changes in aquatic and terrestrial environments with glacial-interglacial climatic cycles. In contrast to other regional pollen records (e.g., Tzedakis et al., 2006; Sadori et al., 2016; Donders et al., 2021; Koutsodendris et al., 2023), the Site M0078 pollen record suggests that Mediterranean and mesophilous vegetation co-dominate in the Corinth Rift area throughout the study interval. In particular, our record highlighted that forested landscapes dominated interglacial intervals, while the region was characterized by open woodlands and grasslands with increased steppic elements during glacials. The interglacial forested landscapes probably acted as a refugium for trees with contrasting ecological niches during glacials (McNeill et al., 2019b; Cullen et al., 2021; Kafetzidou et al., 2023).

Sediment lithology and chemistry also indicate variations in paleoenvironment of the basin (Fig. 4). White laminated packages rich in aragonite are observed at transitions between marine and isolated conditions (Facies M4 and M5, Figs. 4, 7) and are interpreted to represent increased seasonal variability, where aragonite precipitation in late spring/early summer is favored due to increased Mg/Ca from the influx of marine waters over the transition (Gawthorpe et al., 2022). However, detailed study of the MIS5 period suggests there may not be a single set of conditions that explain the aragonite laminations (Sergiou et al., 2024). Distinct periods of fresh, brackish, and marine water have also been interpreted from the sediment chemistry. For example, large variations in magnetic susceptibility from multi-sensor core logger data appear to relate to variations in iron species, with these variations interpreted to be due to change in sulfate availability driven by degree of freshening of the basin water column (Mahoney and März, 2022).

The high sedimentation rates in the Gulf of Corinth have also enabled

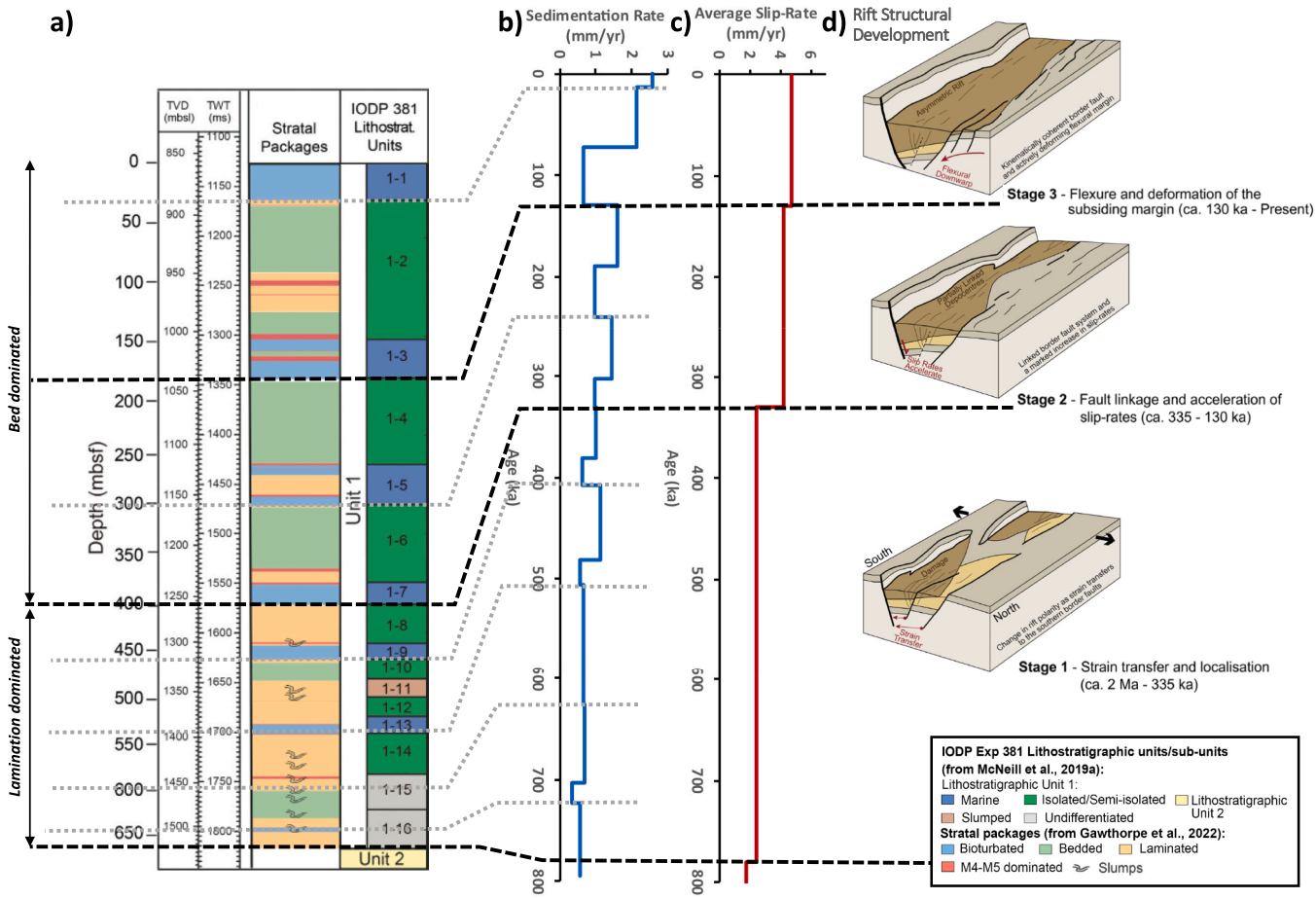

Fig. 7. Synthesis of sedimentary and tectonic processes within the Corinth Rift system, focused on data from Site M0079. a) Site M0079 lithostratigraphic units with stratal packages (from Gawthorpe et al., 2022; Pechlivanidou et al., 2025) and IODP Lithostratigraphic units (from McNeill et al., 2019a; color coding as for Fig. 3 except brown = slumped subunit 1-11 here). Stratal packages are separated into bioturbated, bedded and laminated types. Red bands indicate M4-M5 beds dominate: M4 beds are mud beds with wavy and/or discontinuous laminations, and M5 beds are mud beds with continuous white laminations (Gawthorpe et al., 2022). Identified slump deposits are also marked. Laminated stratal packages dominate at 650–400 mbsf (meters below seafloor), followed by bedded stratal package dominance at 400–180 mbsf. b) Sediment accumulation rates through time for Site M0079 averaged for each lithostratigraphic subunit using all sediments including event beds (after Pechlivanidou et al., 2025; see also McNeill et al., 2019b; Maffione and Herrero-Bervera, 2022; Mohamed et al., 2024). Pattern generally shows higher rates in glacial periods relative to interglacials (with exception of the most recent interglacial). c) Average slip rate of the border fault system through time (Nixon et al., 2024). Note sediment accumulation rates (b) show two broad increases in rate which coincide with increases in average slip rate of the border fault system (c). d) The stages of tectonic development as strain localizes and the border fault develops (see Nixon et al., 2024; Fig. 6). (For interpretation of the references to color in this figure legend, the reader is referred to the web version of this article.)

detailed interpretations of paleoenvironment and paleoclimate in specific intervals (Fig. 7). For example, ostracod assemblages in Site M0080 provide climate and sea level details within the last deglaciation, including recognisable signatures from Heinrich events, Bølling-Allerød interstadials and the Younger Dryas as well as a detailed record of sea level over MIS2–1 (Mazzini et al., 2023).

6. Controls on flux, lithology, and distribution of sediments

The IODP drilling data provide constraints on the ages and lithologies of rift basin sediments, which have been combined with the marine seismic imaging, onshore geological data, and modelling. The combined results reveal substantial temporal and spatial variations in the volume and properties of sediments in the basin (McNeill et al., 2019b; Gawthorpe et al., 2022; Kang et al., 2023; Nixon et al., 2024; Mohamed et al., 2024; Maffione and Herrero-Bervera, 2022; Pechlivanidou et al., 2025), and they illustrate the relative influences of rift faulting versus paleoclimate and paleoenvironment on sediment flux, transport and deposition in rift settings over time.

One of the principal findings of IODP Expedition 381 was the link between paleoclimate and the volume and lithology of basin sediments, with paleoclimate appearing to be the dominant control on ~10s - 100s kyr timescale fluctuations in sedimentation. The new drilling data have enabled calculation of sediment accumulation rates within the rift basin (Fig. 7b). For the most recent phase of rifting, McNeill et al. (2019b) found that sediment accumulation rates are 2–7 times higher during glacials than interglacials. These rates were based on age constraints available from the IODP Expedition 381 Report (McNeill et al., 2019a), a fixed sill depth, and links between the alternating paleoenvironments observed in the cores and the eustatic sea level curve of Spratt and Lisiecki (2016). Subsequent studies have built upon these results with additional constraints on chronology, consideration of sill depth change through time and removal of instantaneous event beds (turbidites) to calculate actual background sedimentation rates (e.g., Maffione and Herrero-Bervera, 2022; Mohamed et al., 2024; Pechlivanidou et al., 2025; Fig. 7b). Although these studies generate some differences in absolute sedimentation rates/sediment accumulation rates, the high rates and the relative difference between glacial (higher rates) and interglacial (lower rates) periods persist. Pollen records in the cores (see above) suggest that climate-driven differences in terrestrial vegetation

may drive these variations via controls on erosion rates, with more densely forested landscapes during interglacials and open woodlands and grasslands during glacials (e.g., McNeill et al., 2019b; Cullen et al., 2021; Kafetzidou et al., 2023).

Sediments deposited during glacials are dominated by bedded packages of mud-dominated hemipelagic sediments and graded beds interpreted to be deposited by low-density turbidity flows, and by laminated beds (Figs. 4, 7a). In contrast, sediments deposited during interglacials are dominated by bioturbated muds (Figs. 4, 7a). The changes in the volume and nature of sedimentation during glacial versus interglacial times are the consequence of changes in paleoenvironment onshore and offshore, including hydrodynamic processes within the basin (Gawthorpe et al., 2022; Kang et al., 2023). The heavily bioturbated muds that characterize interglacials are consistent with a well oxygenated basin permitting abundant marine life similar to today and to the assemblages found in the cores (Gawthorpe et al., 2022). The preservation of bedding in the glacial intervals is linked to reduced bioturbation implying oxygen-depleted bottom waters due to water body stratification. As described above, changing vegetation onshore may have permitted greater erosion during glacial periods (McNeill et al., 2019b), resulting in increased sediment accumulation and potentially more abundant event beds/turbidites during glacials (Gawthorpe et al., 2022). The sediments also record complex basin conditions at transitions between marine (interglacial) and isolated (glacial) periods, which are commonly represented in the cores as sub-mm to mm laminations of calcite or aragonite demonstrating seasonal variability (M4-M5 facies, Figs. 4, 7; Gawthorpe et al., 2022). Similar sediments are found in the adjacent Rion Basin (western end of the Gulf of Corinth) that are also interpreted to reflect climate-eustatic change influencing basin conditions and sedimentation in this more proximal setting (Tsoni et al., 2021).

From combining new drilling data with existing datasets, we interpret that the large-scale distribution of sediments within the basin is controlled by faults along the rift, with the thickest sediments accumulating in a given time interval in the down-dropped hanging wall of faults active during that time period, culminating in deposition in the hanging wall of the now linked border fault system (e.g., Nixon et al., 2016). Changes in fault and rift activity show a clear correlation with the sediment accumulation rates and lithologies within the rift basin (Fig. 7b and c). For example, strain localization and linkage of the border fault system appears to correlate with an increase in sediment accumulation rate in the basin (Fig. 7b; see also Maffione and Herrero-Bervera, 2022) and a change in the character of sediment deposition from lamination-dominated to bedding-dominated stratal packages during lowstand conditions (Fig. 7a; Gawthorpe et al., 2022). As fault activity has evolved and migrated, so too have the sedimentary depocenters, with individual depocenters ultimately merging as faults became linked and focused on the southern rift margin (e.g., Sachpazi et al., 2003; Bell et al., 2009; Taylor et al., 2011; Nixon et al., 2016). Extending the new IODP chronological constraints to the grid of seismic lines in Corinth confirms this relationship and provides more temporal detail and better quantification (Nixon et al., 2024). Despite the high sediment flux rates into the basin, the creation of accommodation space by faulting has still outpaced sediment accumulation over the more recent phase of rifting, such that the basin is underfilled.

Detailed investigations have revealed how fault dip, catchment lithology, and development of individual river-canyon systems influence the dispersal of sediments. Numerical modelling combined with geological data shows how footwall uplift increases erosion and incision but tilting of the footwalls and hanging walls of faults also modulates sediment supply (Pechlivanidou et al., 2019). At the catchment scale, the grain size of materials delivered into the rift is shown to be primarily controlled by catchment lithology and by fluvial morphodynamics, both of which may vary along a rift system, complicating interpretation of the tectonic and environmental controls on sedimentation (Watkins et al., 2020). Integration of the IODP results with new high-resolution seismic data shows that sedimentation patterns during glacial and interglacial periods are strongly controlled by individual canyon systems feeding the rift basin, where steep canyons such as the Sythas Canyon deliver sediment into the basin during both glacial and interglacial times, but other canyon systems shut down during interglacial times (Mohamed et al., 2024).

7. Discussion and Conclusions

IODP Expedition 381 results have yielded a high-resolution record of faulting, sedimentation, and paleoenvironment in an early-stage rift basin. Here we compare results from the Corinth Rift with other rift systems and basins, including rifts at different stages in their evolution, to identify common processes and attributes.

7.1. Rift Development Processes

Integration of borehole chronology with seismic reflection data in the Gulf of Corinth and Alkyonides Gulf illustrates the temporal and spatial evolution of rift faulting (Figs. 6, 7) including: 1) the nature and rate of localization of extension onto border faults; 2) that renewed activity on intrarift faults is due to hanging wall flexure (intrarift faults are smaller faults formed in the hanging wall of border faults); and 3) the importance of rift faults for sedimentary depocenter evolution (Nixon et al., 2024). Results from other active rifts highlight similar fault evolution processes, albeit largely at slower rates and with lower resolution constraints than in Corinth. Many rifts and rift models show a localization of extension onto border faults over time, some with increased extension (e.g., Ebinger and Casey, 2001; Cowie et al., 2005; Ebinger, 2012; Brune et al., 2023). For example, the most immature segments of the Western Rift of the East Africa Rift System (EARS) (e.g., southern Malawi Rift; Wedmore et al., 2020) show that extension is distributed across intrarift faults and incipient border faults (strain not yet localized). In the Whakatane Graben, New Zealand, a rift system of similar scale and age to Corinth albeit opening at much lower rates of extension and strain, gradual localization onto a single linked border fault was also accompanied by a 3-fold increase in its slip rate (Taylor et al., 2004), as observed in Corinth (Nixon et al., 2024; Figs. 6,7). We note that acceleration of extension has also been identified in mature rift systems but occurs later in the rift process and over a longer time period than observed in Corinth (compare with Atlantic Ocean examples in Brune et al., 2016). In more mature rift systems, such as the North Sea and Suez Rift and in some more mature segments of the East African Rift System, progressive localization of strain from an array of distributed faults to one or more well-linked fault systems such as a border fault system has also been interpreted (e.g., Gawthorpe et al., 2003; Cowie et al., 2005; Muirhead et al., 2019; Scholz et al., 2020). In the case of the Corinth system, the high rates of process and rapidity of reaching this stage of localization are unusual relative to the start of rifting and to continental breakup, and this raises questions about the nature of the next evolutionary phase of the border fault system and basin subsidence in this rift and in general.

The timing of enhanced intrarift fault activity may be common between rifts, even if controls on this activity vary between rifts. In the Corinth Rift, intrarift faults show a significant increase in activity during the most recent phase of rifting, which is coincident with and interpreted to result from linkage of the border fault system and increased hanging wall flexure as displacement has accrued on these border faults (Nixon et al., 2024). Hanging wall flexure is also proposed to contribute to recent activity on intra-rift faults in the northern Malawi Rift (Biggs et al., 2010; Shillington et al., 2020; Wright et al., 2023). In contrast, in magmatic rift systems, such as the Eastern Branch of the East African Rift System and rift basins along the margins of the Atlantic Ocean, increased intrarift fault activity occurred during later stages of basin development and is linked to magmatism (e.g., Muirhead et al., 2016; Withjack et al., 2024). Constraints on the spatiotemporal evolution of rift faulting at

comparable resolution to those now available in Corinth are also needed in magmatic rifts to enable further comparisons and understanding of the drivers and timings of intrarift fault activity.

The constraints on the spatiotemporal evolution of faulting in the Corinth Rift make it an excellent case study to compare with other rifts and to constrain rift models (e.g., Cowie et al., 2005; Brune et al., 2023). In general, quantified rates of process in rift systems at high resolution are rare, and the new Corinth dataset is therefore an important addition.

7.2. Paleoclimate and Paleoenvironment of Tectonic Basins

The IODP Expedition 381 (Corinth Rift) results reveal unexpected level of variability over very short timescales of 10s kyr or less in basin paleoenvironment driven by changes in eustatic sea level with respect to basin sills and climate, in particular at the transitions between marine/interglacial and isolated/glacial conditions (e.g., McNeill et al., 2019b; Gawthorpe et al., 2022; Sergiou et al., 2024; Pechlivanidou et al., 2025; Fatourou et al., 2025; Figs. 3–5, 7). Significant shifts in sea-surface productivity, salinity, and temperatures recorded by dinoflagellate cysts correspond to orbitally-driven climatic variability (Fatourou et al., 2025). The pollen record from Expedition 381 suggests the occurrence of a largely forested landscape with varying forest composition and periods of woodland opening (a shift from more dense forest/woodland to less dense tree cover) during glacial intervals. The continuous occurrence of mesophilous tree vegetation suggests that, even during glacial intervals, moisture availability was not limiting their growth in the borderlands of the Gulf (e.g., Kafetzidou et al., 2023; Fig. 5). Drilling data elsewhere show that other tectonic basins have also experienced alternating basin paleoenvironments due to interactions of tectonics and climate (e.g., Sea of Marmara, Black Sea, Caspian Sea; Hsü, 1978; McHugh et al., 2008; Aksu and Hiscott, 2022). However, these records tend to have a lower resolution and greater chronological uncertainty (e.g., Krijgsman et al., 2019). The other active, early-stage rift with well-resolved constraints on paleoenvironment (although without ocean connection) is the Malawi Rift in the southern part of the East African Rift System. International Continental Drilling Program (ICDP) drilling here revealed marked changes in lake level, basin environment and rift-flank vegetation driven by climate (Lyons et al., 2015). However, the frequency and specific drivers for hydroclimatic changes in this land-locked lake in sub-Saharan Africa not surprisingly differ from those in the Mediterranean (Scholz et al., 2007; Lyons et al., 2015).

Although all rifts and restricted basins are likely to be highly sensitive to climate variations, the specific patterns will vary depending on their latitude, regional climate and level of ocean connectivity. Regardless of regional setting, the particularly high-resolution record from the Corinth Rift provides an important point of comparison for other basins in tectonically active areas that experience alternating environments, with particularly interesting results on the rate and style of change during transitional times (e.g., Sergiou et al., 2024).

7.3. Sedimentary processes

The record of sedimentation from IODP Expedition 381 exemplifies how tectonic and climatic processes combine to shape the rate and lithology of sediment accumulation in young rift basins. The sediment accumulation rates in the Corinth Rift basins are very high, at up to 3–4 mm/yr (McNeill et al., 2019b; Pechlivanidou et al., 2025; Fig. 7b); only the northern Gulf of California and Sea of Marmara have comparable rates of 2–4 mm/yr (McHugh et al., 2008; Dorsey, 2010). These exceptionally high sedimentation rates enable us to resolve the geologic and stratigraphic history of the Corinth rift at high resolution. These rates could also be applied to the deeply buried parts of mature rifts with similar pre-breakup extension rates, e.g., the South Atlantic (Brune et al., 2016), to predict and assess their early sedimentation patterns.

It has long been recognized that large-scale and longer term patterns of sediment accumulation in the Corinth Rift are controlled by extensional processes, with major depocenters controlled by primary rift faults (e.g., Bell et al., 2009; Nixon et al., 2016; Nixon et al., 2024). This is also observed in many other active and ancient rifts (East Africa – Morley, 1999; primarily active rifts - Gawthorpe and Leeder, 2000; Suez rift - Gawthorpe et al., 2003; Lake Malawi - Scholz et al., 2020; North American Atlantic margin - Withjack et al., 2024). This is shown in Corinth by the increases in slip rates on the border fault system correlating with increases in long term sediment accumulation rate through time (Fig. 7b & 7c). Such a correlation between tectonic activity and sediment accumulation rate is also evident in the earlier rift history of Corinth (where low sedimentation rates, 0.4-0.7 mm/yr, are correlated with low extension rates, 1.1-2.0 mm/yr, on the earliest western Corinth Rift margin; Hemelsdaël et al., 2021). Expedition 381 cores also provide new insights into how sedimentary processes and lithologies are connected to tectonic processes in rifts; for example, the change in the character of sediment deposition from lamination dominated to bedding dominated (associated with increased gravity flow deposits) during lowstands coincides with the linkage, localization, and slip-rate acceleration on the border fault system at ca. 330 ka (Fig. 7a). This may be due to more rapid subsidence in the fault hanging walls and subsequent steepening of basin slopes. Similarly, increases in subsidence and steepening slopes have been shown to enhance gravity flows both locally and into the wider basin during lowstands in the North Sea rift (Carruthers et al., 1996).

The Corinth Rift also exhibits variations in sediment types, volumes and sedimentary processes at higher frequencies and on smaller spatial scales. These variations arise from a wide range of processes in and around the basin, including changes in fault activity, temperature, precipitation, sea level fluctuation, sediment flux and amount and type of vegetation cover affecting erosion (e.g., McNeill et al., 2019b; Pechlivanidou et al., 2019; Gawthorpe et al., 2022; Sergiou et al., 2024; Mohamed et al., 2024). The high-resolution record from IODP Expedition 381 provides a unique opportunity to parse the relative importance and interplay of these controls. For example, one of the most striking new results from Expedition 381 is the contrast in sediment type and process between glacial and interglacial periods and as the basin becomes better connected to the open marine Mediterranean as the rift subsides and/or basin sills lower (Figs. 3–5, 7). This includes changes in lithology and stratal package type (bioturbated vs bedded vs laminated; Fig. 4), sediment transport processes reflecting the changing hydrological basin conditions, sediment geochemistry, and sediment accumulation rate with higher rates of sedimentation occurring during glacial periods (McNeill et al., 2019b; Gawthorpe et al., 2022; Sergiou et al., 2024; Pechlivanidou et al., 2025; Fig. 7b). Cyclicity in sedimentation patterns has also been observed in the tropical, lacustrine Malawi and Tanganyika Rifts and is interpreted to result from alternations between dry periods with significant lake evaporation and wetter periods (Cohen et al., 1997; Scholz et al., 1998).

Overall, the IODP drilling results from the Corinth Rift provide us with a new high-resolution record of how an early rift develops and how tectonic, sedimentary and environmental processes interact at a resolution not available until now. Such information will provide an important record for testing numerical models and increasing our understanding of other rift systems at various stages of maturity. Obtaining comparable drilling and geophysical data from other rift systems at different stages in their evolution, formed in different geodynamical contexts, and developing in different climates is needed to further advance our understanding.

CRediT authorship contribution statement

Lisa C. McNeill: Writing – review & editing, Writing – original draft, Project administration, Investigation, Funding acquisition, Conceptualization. **Donna J. Shillington:** Writing – review & editing, Writing – original draft, Project administration, Investigation, Conceptualization. **Jeanine Ash:** Writing – review & editing, Investigation. **Gareth D.O.**

Carter: Writing – review & editing, Project administration, Investigation. **Richard E.Ll. Collier:** Writing – review & editing, Investigation. **Aleksandra Cvetkoska:** Writing – review & editing, Investigation. **Paula Diz:** Writing – review & editing, Investigation. **Mai-Linh Doan:** Writing – review & editing, Investigation. **Jeremy D. Everest:** Project administration. **Natacha Fabregas:** Writing – review & editing, Investigation. **Eugenia Fatourou:** Writing – review & editing, Investigation. **Mary Ford:** Writing – review & editing, Investigation. **Robert L. Gawthorpe:** Writing – review & editing, Investigation. **Gino De Gelder:** Writing – review & editing, Investigation. **Maria Geraga:** Writing – review & editing, Investigation. **Jack Gillespie:** Writing – review & editing, Investigation. **Sophie Green:** Project administration. **Romain Hemelsdaël:** Writing – review & editing, Investigation. **Emilio Herrero-Bervera:** Writing – review & editing, Investigation. **Mohammad Ismaiel:** Writing – review & editing, Investigation. **Liliane Janikian:** Writing – review & editing, Investigation. **Cari Johnson:** Writing – review & editing, Investigation. **Aikaterini Kafetzidou:** Writing – review & editing, Investigation. **Olga Koukousioura:** Writing – review & editing, Investigation. **Katerina Kouli:** Writing – review & editing, Investigation. **Erwan Le Ber:** Investigation. **Shunli Li:** Writing – review & editing, Investigation. **Marco Maffione:** Writing – review & editing, Investigation. **Carol Mahoney:** Writing – review & editing, Investigation. **Malka L. Machlus:** Writing – review & editing, Investigation. **Fabienne Marret:** Writing – review & editing, Investigation. **Ilaria Mazzini:** Writing – review & editing, Investigation. **Georgios Michas:** Writing – review & editing, Investigation. **Clint Miller:** Investigation. **Casey W. Nixon:** Writing – review & editing, Investigation. **Sabire Asli Oflaz:** Investigation. **Abah P. Omale:** Writing – review & editing, Investigation. **Konstantinos Panagiotopoulos:** Writing – review & editing, Investigation. **Roberta Parisi:** Writing – review & editing, Investigation. **Sofia Pechlivanidou:** Writing – review & editing, Investigation. **Marcie Purkey Phillips:** Writing – review & editing, Investigation. **Simone Sauer:** Investigation. **Joana Seguin:** Writing – review & editing, Investigation. **Spyros Sergiou:** Writing – review & editing, Investigation. **Natalia V. Zakharova:** Writing – review & editing, Investigation.

Declaration of competing interest

The authors declare the following financial interests/personal relationships which may be considered as potential competing interests:

Lisa McNeill, Richard Collier, Marco Maffione, Carol Mahoney report financial support was provided by UK Research and Innovation Natural Environment Research Council. Katerina Kouli, Eugenia Fatourou, Aikaterini Kafetzidou report financial support was provided by Hellenic Foundation of Research and Innovation. Robert Gawthorpe, Sofia Pechlivanidou, Natacha Fabregas report financial support was provided by Research Council of Norway (NFR). Robert Gawthorpe, Sofia Pechlivanidou, Natacha Fabregas, Casey Nixon report financial support was provided by Norwegian Academy of Science and Letters. Ilaria Mazzini, Roberta Parisi report financial support was provided by CNR ECORD-IODP e ICDP, Italia. Olga Koukousioura, Kostas Panagiotopoulos report financial support was provided by Deutsche Forschungsgemeinschaft. Mary Ford, Mai-Linh Doan, Gino de Gelder, Simone Sauer, Romain Hemelsdael report financial support was provided by IODP France. Kostas Panagiotopoulos, Sabire Asli Oflaz, Joana Seguin, Aleksandra Cvetkoska report financial support was provided by IODP Germany (DFG). Liliane Janikian reports financial support was provided by CAPES Brazil. Donna Shillington, Jeanine Ash, Emilio Herrero-Bervera, Malka Machlus, Clint Miller, Abah Omale, Marcie Purkey Phillips, Natalia, Zakharova, Cari Johnson report financial support was provided by United States Science Support Program (IODP). Lisa McNeill, Richard Collier, Marco Maffione, Carol Mahoney report financial support was provided by UKIODP NERC. Mohammad Ismaiel reports financial support was provided by IODP India. Jack Gillespie reports financial support was provided by IODP ANZIC. If there are other authors, they declare that they have no known competing financial interests or personal relationships that could have appeared to influence the work reported in this paper.

Acknowledgements

We sincerely thank all involved with the completion of IODP Expedition 381, including ECORD Science Operator staff, ship and drilling crew of the D/V *Fugro Synergy*, and staff at MARUM, University of Bremen. We thank Tom Cronin for his considerable contributions to Expedition 381 and subsequent research. We thank national and local funding agencies that provided support for all the co-authors during their research. LM acknowledges funding from the UK Natural Environment Research Council (NERC) (NE/R016550/1, NE/J006564/1). RC acknowledges funding from the NERC (NE/S002367/1). MM acknowledges funding from the NERC (NE/R013942/1). CMa acknowledges funding from the NERC (NE/R018170/1). KK, AK and EF acknowledge funding from the Hellenic Foundation of Research and Innovation (H.F.R.I) (PN: 1026). RG and SP acknowledge funding from the Research Council of Norway (NFR) (PN: 308805). RG, SP, CN and NF acknowledge funding from the VISTA programme of the Norwegian Academy of Science and Letters. RP and IM acknowledge funding from CNR ECORD-IODP e ICDP commission through MUR for ECORD-IODP Italia. OK and KP acknowledge funding from the Deutsche Forschungsgemeinschaft (DFG) (GR 5285/3-1, PA 2664/8-1). MF, MD, RH, GG and SSa acknowledge funding from IODP-France. KP, SAO, JS, AC acknowledge funding from IODP Germany DFG. LJ acknowledges funding from CAPES Brazil (23038.007096/2017-61). DS, JA, EHB, MLM, CMi, AO, MPP, NZ, CJ acknowledge funding from IODP USSSP (USA). LM, RC, MM, CMa acknowledge funding from UKIODP NERC. MI acknowledges funding from IODP India. SL acknowledges funding from IODP China. JG acknowledges support from IODP ANZIC.

We thank Robert Poirier and Whittney Spivey for earlier comments, and Tiago Alves and an anonymous reviewer for constructive comments that improved the paper.

Data availability

The data generated from IODP Expedition 381 are openly available. Drill core data are available at: https://iodp.pangaea.de/. Logging data are available at: https://mlp.ldeo.columbia.edu/logdb/scientific_ocean_drilling/. Datasets generated from published material described in this publication are available from each publication in the form of supplementary material.

References

Aksu, A.E., Hiscott, R.N., 2022. Persistent Holocene outflow from the Black Sea to the eastern Mediterranean Sea still contradicts the Noah's Flood Hypothesis: a review of 1997–2021 evidence and a regional paleoceanographic synthesis for the latest Pleistocene–Holocene. Earth-Sci. Rev. 227. https://doi.org/10.1016/j.earscirev.2022.103960.

Avallone, A., Briole, P., Agatza-Balodimou, A.M., Billiris, H., Charade, O., Mitsakaki, C., Nercessian, A., Papazissi, K., Paradissis, D., Veis, G., 2004. Analysis of eleven years of deformation measured by GPS in the Corinth Rift Laboratory area. Compt. Rendus Geosci. 336 (4–5), 301–311. https://doi.org/10.1016/j.crte.2003.12.007.

Bastow, I.D., Booth, A.D., Corti, G., Keir, D., Magee, C., Jackson, C.A.-L., et al., 2018. The development of late-stage continental breakup: Seismic reflection and borehole evidence from the Danakil Depression, Ethiopia. Tectonics 37 (9), 2848–2862. https://doi.org/10.1029/2017TC004798.

Bayrakci, G., Minshull, T.A., Sawyer, D.S., Reston, T.J., Klaeschen, D., Papenberg, C., Ranero, C., Bull, J.M., Davy, R.G., Shillington, D.J., Perez-Gussinye, M., Morgan, J. K., 2016. Fault-controlled hydration of the upper mantle during continental rifting. Nat. Geosci. 9, 384–388.

Bell, R.E., McNeill, L.C., Bull, J.M., Henstock, T.J., Collier, R.E.L., Leeder, M.R., 2009. Fault architecture, basin structure and evolution of the Gulf of Corinth, central Greece. Basin Res. 21, 824–855. https://doi.org/10.1111/j.1365-2117.2009.00401.x.

Bell, R.E., Jackson, C.A.L., Whipp, P.S., Clements, B., 2014. Strain migration during multiphase extension: Observations from the northern North Sea. Tectonics 33, 1936–1963. https://doi.org/10.1002/2014TC003551.

Biggs, J., Nissen, E., Craig, T., Jackson, J., Robinson, D.P., 2010. Breaking up the hanging wall of a rift-border fault: The 2009 Karonga earthquakes, Malawi. Geophys. Res. Lett. 37, L11305, 11310.11029/12010GL043179.

Brune, S., Williams, S., Butterworth, N., et al., 2016. Abrupt plate accelerations shape rifted continental margins. Nature 536, 201–204. https://doi.org/10.1038/nature18319.

Brune, S., Kolawole, F., Olive, J.-A., Stamps, D.S., Buck, W.R., Buiter, S.J.H., Furman, T., Shillington, D.J., 2023. Geodynamics of continental rift initiation and evolution. Nat. Rev. Earth Environ. 4, 235–253. https://doi.org/10.1038/s43017-023-00391-3.

Carruthers, A., McKie, T., Price, J., Dyer, R., Williams, G., Watson, P., 1996. The application of sequence stratigraphy to the understanding of Late Jurassic turbidite plays in the Central North Sea, UKCS. Geol. Soc. Lond. Spec. Publ. 114, 29–45.

Cohen, A.S., Lezzar, K.-E., Tiercelin, J.-J., Soreghan, M., 1997. New palaeogeographic and lake-level reconstructions of Lake Tanganyika: implications for tectonic, climatic and biological evolution in a rift lake. Basin Res. 9, 107–132.

Collier, R.E.L., Leeder, M.R., Trout, M., Ferentinos, G., Lyberis, E., Papatheodorou, G., 2000. High sediment yields and cool, wet winters: test of last glacial paleoclimates in the northern Mediterranean. Geology 28, 999–1002. https://doi.org/10.1130/0091-7613(2000)28<999:HSYACW>2.0.CO;2.

Cowie, P.A., Underhill, J., Behn, M., Lin, J., Gill, C., 2005. Spatio-temporal evolution of strain accumulation derived from multi-scale observations of Late Jurassic rifting in the northern North Sea: a critical test of models for lithospheric extension. Earth Planet. Sci. Lett. 234, 401–419. https://doi.org/10.1016/j.epsl.2005.01.039.

Cowie, P.A., Roberts, G.P., Mortimer, E., 2007. Strain localization within fault arrays over timescales of 10^0–10^7 years. In: Handy, M.R., Hirth, G., Hovius, N. (Eds.), Tectonic Faults: Agents of Change on a Dynamic Earth. MIT Press, pp. 47–78.

Cullen, T.M., Collier, R.E.L., Hodgson, D.M., Gawthorpe, R.L., Kouli, K., Maffione, M., Kranis, H., Eliassen, G.T., 2021. Deep-water syn-rift stratigraphy as archives of Early-Mid Pleistocene palaeoenvironmental signals and controls on sediment delivery. Front. Earth Sci. 9. https://doi.org/10.3389/feart.2021.715304.

De Gelder, G., Doan, M.L., Beck, C., Carlut, J., Seibert, C., Feuillet, N., Carter, G.D.O., Pechlivanidou, S., Gawthorpe, R.L., 2021. Multi-scale and multi-parametric analysis of Late Quaternary event deposits within the active Corinth Rift (Greece). Sedimentology 69, 1573–1598. https://doi.org/10.1111/sed.12964.

Donders, T., Panagiotopoulos, K., Koutsodendris, A., Bertini, A., Maria Mercuri, A., Masi, A., Combourieu-Nebout, N., Joannin, S., Kouli, K., Kousis, I., et al., 2021. 1.36 Million Years of Mediterranean Forest Refugium Dynamics in Response to Glacial-Interglacial Cycle Strength. Proc. Natl. Acad. Sci. USA 118, e2026111118.

Dorsey, R., 2010. Sedimentation and crustal recycling along an active oblique-rift margin: Salton Trough and northern Gulf of California. Geology 38, 443–446.

Dorsey, R.J., Umhoefer, P.J., 2000. Tectonic and eustatic controls on sequence stratigraphy of the Pliocene Loreto basin, Baja California Sur. Mexico. Geol. Soc. Am. Bull. 112, 177–199. https://doi.org/10.1130/0016-7606(2000)112<177:TAECOS>2.0.CO;2.

Ebinger, C.J., 2012. Evolution of the Cenozoic East African rift system: Cratons, plumes, and continental breakup. In: Roberts, D.G., Bally, A.W. (Eds.), Phanerozoic Rift Systems and Sedimentary Basins. Elsevier, pp. 133–162 doi:110.1016/B1978–1010–1444–56356-56359.00006-56357.

Ebinger, C.J., Casey, M., 2001. Continental breakup in magmatic provinces: An Ethiopian example. Geology 29 (6), 527–530.

Ebinger, C., Scholz, C.A., 2012. Continental rift basins: The East African perspective. In: Busby, C, Azor, A. (Eds.), Tectonics of Sedimentary Basins: Recent Advances, pp. 183–208.

Fatourou, E., Kafetzidou, A., Marret, F., Panagiotopoulos, K., Kouli, K., 2023. Late Quaternary Ponto-Caspian dinoflagellate cyst assemblages from the Gulf of Corinth, Central Greece (eastern Mediterranean Sea). Mar. Micropaleontol. 179, 102211. https://doi.org/10.1016/j.marmicro.2023.102211.

Fatourou, E., Kafetzidou, A., Marret, F., Panagiotopoulos, K., Kouli, K., 2025. Paleoceanographic evolution of the Gulf of Corinth (Greece) during Quaternary glacial-interglacial cycles. Quat. Sci. Rev. 360, 109393. https://doi.org/10.1016/j.quascirev.2025.109393.

Follieri, M., Magri, D., Sadori, L., 1989. Pollen stratigraphical synthesis from Valle di Castiglione (Roma). Quat. Int. 3–4, 81–84.

Ford, M., Rohais, S., Williams, E.A., Bourlange, S., Jousselin, D., Backert, N., Malartre, F., 2013. Tectono-sedimentary evolution of the western Corinth rift (Central Greece). Basin Res. 25 (1), 3–25. https://doi.org/10.1111/j.1365-2117.2012.00550.x.

Ford, M., Hemelsdael, R., Mancini, M., Palyvos, N., 2017. Rift migration and lateral propagation: evolution of normal faults and sediment routing systems of the western Corinth. Rift (Greece). In: Childs, C., Holdsworth, R.E., Jackson, C.A.-L., Manzocchi, T., Walsh, J.J., Yielding, G. (Eds.), The Geometry and Growth of Normal Faults, Geological Society, London. https://doi.org/10.1144/SP439.15. Special Publication 439.

Gawthorpe, R.L., Leeder, M.R., 2000. Tectono-sedimentary evolution of active extensional basins. Basin Res. 12 (3–4), 195–218.

Gawthorpe, R.L., Hurst, J.M., Sladen, C.P., 1990. Evolution of Miocene footwall-derived coarse grained deltas, Gulf of Suez, Egypt: implications for exploration. Am. Ass. Petrol. Geol. Bull. 74, 1077–1086.

Gawthorpe, R.L., Jackson, C.A.L., Young, M.J., Sharp, I.R., Moustafa, A.R., Leppard, C. W., 2003. Normal fault growth, displacement localisation and the evolution of normal fault populations: the Hammam Faraun fault block, Suez rift. Egypt. J. Struct. Geol. 25, 883–895. https://doi.org/10.1016/S0191-8141(02)00088-3.

Gawthorpe, R.L., Leeder, M.R., Haralambos, K., Skourtsos, E., Andrews, J.E., Henstra, G. A., Mack, G.H., Muravchik, M., Turner, J.A., Stamatakis, M., 2018. Tectono-sedimentary evolution of the Plio-Pleistocene Corinth rift, Greece. Basin Res. 30, 448–479. https://doi.org/10.1111/bre.12260.

Gawthorpe, R.L., Fabregas, N., Pechlivanidou, S., Ford, M., Collier, R.E.L., Carter, G.D.O., McNeill, L.C., Shillington, D.J., 2022. Late Quaternary mud-dominated, basin-floor sedimentation of the Gulf of Corinth, Greece: Implications for deep water depositional processes and controls on sedimentation. Basin Res. 34, 1567–1600. https://doi.org/10.1111/bre.12671.

Hemelsdaël, R., Charreau, J., Ford, M., Proborukmi, M.S., Malartre, F., Urban, B., Blard, P.-H., 2021. Tectono-climatic controls of the early rift alluvial succession: Plio-Pleistocene Corinth Rift (Greece). Paleogeography, Paleoclimatology, Paleoecology 576, 110507.

Hemelsdaël, R., Gawthorpe, R., Pechlivanidou, S., Hatletvedt, K.O., Bruguier, O., 2024. Early rift development and palaeo-environments of the easternmost part of Corinth rift (Greece): IODP Expedition 381 Site M0080. In: International Association of Sedimentologists Conference, Aberdeen, UK.

Hsü, K.J., 1978. Stratigraphy of the lacustrine sedimentation in the Black Sea. In Deep Sea Drilling Project Initial Reports 42, 509–524.

Kafetzidou, A., Fatourou, E., Panagiotopoulos, K., Marret, F., Kouli, K., 2023. Vegetation composition in a typical Mediterranean setting (Gulf of Corinth, Greece) during successive Quaternary climatic cycles. Quaternary 6 (2), 30. https://doi.org/10.3390/quat6020030.

Kang, W., Li, S., Gawthorpe, R.L., Ford, M., Collier, R.E.L., Yu, X., Janikian, L., Nixon, C. W., Hemelsdaël, R., Sergiou, S., Gillespie, J., Pechlivanidou, S., Gelder, G.D., 2023. Grain-size analysis of the Late Pleistocene sediments in the Corinth Rift: insights into strait-influenced hydrodynamics and provenance of an active rift basin. In: Rossi, V. M., Longhitano, S.G., Olariu, C., Chiocci, F.L. (Eds.), Straits and Seaways: Controls, Processes and Implications in Modern and Ancient Systems. Special Publication - Geological Society of London, 523, pp. 255–277.

Koutsodendris, A., Dakos, V., Fletcher, W.J., et al., 2023. Atmospheric CO2 forcing on Mediterranean biomes during the past 500 kyrs. Nat. Commun. 14, 1664. https://doi.org/10.1038/s41467-023-37388-x.

Krijgsman, W., Tesakov, A., Yanina, T., Lazarev, S., Danukalova, G., Van Baak, C.G.C., Agustí, J., Alçiçek, M.C., Aliyeva, E., Bista, D., Bruch, A., Büyükmeriç, Y., Bukhsianidze, M., Flecker, R., Frolov, P., Hoyle, T.M., Jorissen, E.L., Kirscher, U., Koriche, S.A., Wesselingh, F.P., 2019. Quaternary time scales for the Pontocaspian domain: Interbasinal connectivity and faunal evolution. Earth Sci. Rev. 188, 1–40. https://doi.org/10.1016/j.earscirev.2018.10.013.

Lathrop, B.A., Jackson, C.A.-L., Bell, R.E., Rotevatn, A., 2022. Displacement/Length Scaling Relationships for Normal Faults; a Review, Critique, and Revised Compilation. Front. Earth Sci. 10, 907543. https://doi.org/10.3389/feart.2022.907543.

Lei, C., Alves, T., Ren, J., Tong, C., 2020. Rift Structure and Sediment Infill of Hyperextended Continental Crust: Insights From 3D Seismic and Well Data (Xisha Trough, South China Sea). J. Geophys. Res. 125. https://doi.org/10.1029/2019JB018610 e2019JB018610.

Lykousis, V., Sakellariou, D., Moretti, I., Kaberi, H., 2007. Late Quaternary basin evolution of the Gulf of Corinth: Sequence stratigraphy, sedimentation, fault–slip and subsidence rates. Tectonophysics 440 (1–4), 29–51. https://doi.org/10.1016/j.tecto.2006.11.007.

Lyons, R.P., Scholz, C.A., Cohen, A.S., King, J.W., Brown, E.T., Ivory, S.J., Johnson, T.C., Deino, A.L., Reinthal, P.N., McGlue, M.M., Blome, M.W., 2015. Continuous 1.3-million-year record of East African hydroclimate, and implications for patterns of evolution and biodiversity. PNAS 112, 15568–15573.

Maffione, M., Herrero-Bervera, E., 2022. A relative paleointensity (RPI)-calibrated age model for the Corinth syn-rift sequence at IODP Hole M0079A (Gulf of Corinth, Greece). Front. Earth Sci. 10. https://doi.org/10.3389/feart.2022.813958.

Mahoney, C., März, C., 2022. Tracing glacial-interglacial water mass changes in the Gulf of Corinth (IODP Expedition 381) using iron-sulphur geochemistry and magnetic susceptibility. Mar. Geol. 448, 106801. https://doi.org/10.1016/j.margeo.2022.106801.

Marret, F., Mudie, P., Aksu, A., Hiscott, R.N., 2009. A Holocene dinocyst record of a two-step transformation of the Neoeuxinian brackish water lake into the Black Sea. Quat. Int. 197, 72–86.

Mazzini, I., Cronin, T.M., Gawthorpe, R.L., Collier, R.E.L., de Gelder, G., Golub, A.R., Toomey, M.R., Poirer, R.K., Huang, H.-H.M., Phillips, M.P., McNeill, L.C., Shillington, D.J., 2023. A new deglacial climate and sea-level record from 20 to 8 ka from IODP381 site M0080, Alkyonides Gulf, eastern Mediterranean. Quat. Sci. Rev. 313, 108192.

McHugh, C., Gurung, D., Giosan, L., Ryan, W.B.F., Mart, Y., Sancar, U., Burckle, L., Cagatay, M.N., 2008. The last reconnection of the Marmara Sea (Turkey) to the World Ocean: A paleoceanographic and paleoclimatic perspective. Mar. Geol. 255, 64–82. https://doi.org/10.1016/j.margeo.2008.07.005.

McNeill, L.C., Shillington, D.J., Carter, G.D.O., and the Expedition 381 Participants (2019a). Corinth Active Rift Development. Proceedings of the International Ocean Discovery Program, 381: College Station, TX (International Ocean Discovery Program). doi:10.14379/iodp.proc.381.2019.

McNeill, L.C., Shillington, D.J., Carter, G.D.O., et al., 2019b. High-resolution record reveals climate-driven environmental and sedimentary changes in an active rift. Sci. Rep. 9, 3116. https://doi.org/10.1038/s41598-019-40022-w.

Mohamed, M.A., Collier, R.E.L., Hodgson, D.M., Gawthorpe, R., Shillington, D.J., Muravchik, M., Sakellariou, D., 2024. Sediment flux variation as a record of climate change in a late Quaternary deep-water active rift basin. Basin Res. 36, e12896. https://doi.org/10.1111/bre.12896.

Moretti, I., Lykousis, V., Sakellariou, D., Reynaud, J.-Y., Benziane, B., Prinzhoffer, A., 2004. Sedimentation and subsidence rate in the Gulf of Corinth: What we learn from the Marion Dufresne's long piston coring. Compt. Rendus Geosci. 336, 291–299. https://doi.org/10.1016/j.crte.2003.11.011.

Morley, C.K., 1999. Patterns of displacement along large normal faults: implications for basin evolution and fault propagation, based on examples from east Africa. Am. Assoc. Pet. Geol. Bull. 83, 613–634.

Mudie, P.J., Marret, F., Mertens, K.N., Shumilovskikh, L., Leroy, S.A.G., 2017. Atlas of modern dinoflagellate cyst distributions in the Black Sea Corridor: from Aegean to Aral Seas, including Marmara, Black, Azov and Caspian Seas. Mar. Micropaleontol. 134, 1–152.

Muirhead, J.D., Kattenhorn, S.A., Lee, H., Mana, S., Turrin, B.D., Fischer, T.P., Kianji, G., Dindi, E., Stamps, D.S., 2016. Evolution of upper crustal faulting assisted by magmatic volatile release during early-stage continental rift development in the East African Rift. Geosphere 12 (6), 1670–1700.

Muirhead, J.D., Wright, L.J.M., Scholz, C.A., 2019. Rift evolution in regions of low magma input in East Africa. Earth Planet. Sci. Lett. 506, 322–346.

Muñoz-Barrera, J.M., Rotevatn, A., Gawthorpe, R.L., Henstra, G., Kristensen, T.B., 2021. Supradetachment basins in necking domains of rifted margins: Insights from the Norwegian Sea. Basin Res. 34, 991–1019. https://doi.org/10.1111/bre.12648.

Naliboff, J.B., Buiter, S.J.H., Péron-Pinvidic, G., et al., 2017. Complex fault interaction controls continental rifting. Nat. Commun. 8, 1179. https://doi.org/10.1038/s41467-017-00904-x.

Nixon, C.W., McNeill, L.C., Bull, J.M., Bell, R.E., Gawthorpe, R.L., Henstock, T.J., Christodoulou, D., Ford, M., Taylor, B., Sakellariou, D., Ferentinos, G., Papatheodorou, G., Leeder, M.R., Collier, R., Goodliffe, A.M., Sachpazi, M., Kranis, H., 2016. Rapid spatiotemporal variations in rift structure during development of the Corinth Rift, central Greece. Tectonics 35 (5), 1225–1248. https://doi.org/10.1002/2015tc004026.

Nixon, C.W., McNeill, L.C., Gawthorpe, R.L., Shillington, D.J., Michas, G., Bell, R.E., Moyles, A., Ford, M., Zakharova, N.V., Bull, J.M., de Gelder, G., 2024. Increasing fault slip rates within the Corinth Rift, Greece: A rapidly localising active rift fault network. Earth Planet. Sci. Lett. 636, 118716. https://doi.org/10.1016/j.epsl.2024.118716.

Olive, J.-A., Behn, M.D., Malatesta, L.C., 2014. Modes of extensional faulting controlled by surface processes. Geophys. Res. Lett. 41, 6725–6733.

Pan, S., Naliboff, J., Bell, R., Jackson, C., 2022. Bridging Spatiotemporal Scales of Normal Fault Growth During Continental Extension Using High-Resolution 3D Numerical Models. Geochem. Geophys. Geosyst. 23 e2021GC010316.

Parisi, R., Cronin, T.M., Aiello, G., Barra, D., Danielopol, D.L., Horne, D.J., Mazzini, I., 2024. A new species of benthic ostracod Tuberoloxoconcha: A proxy for glacioeustatic sea-level changes in the Gulf of Corinth. Palaeogeogr. Palaeoclimatol. Palaeoecol. 655, 112483. https://doi.org/10.1016/j.palaeo.2024.112483.

Parisi, R., Cronin, T.M., Tur, N., Toomey, M., Mazzini, I., 2025. Paleoecology and paleoceanography of the Gulf of Corinth revealed by ostracod assemblages. Quat. Sci. Rev. 366, 109489. https://doi.org/10.1016/j.quascirev.2025.109489.

Pechlivanidou, S., Cowie, P.A., Duclaux, G., Nixon, C.W., Gawthorpe, R.L., Salles, T., 2019. Tipping the balance: shifts in sediment production in an active rift setting. Geology 47, 259–262. https://doi.org/10.1130/G45589.45581.

Pechlivanidou, S., Muravchik, M., Gawthorpe, R.L., De Gelder, G., Oflaz, S.A., Collier, R. E.L., Gillespie, J., Machlus, M.L., Maffione, M., Herrero-Bervera, E., Ford, M., Fabregas, N., Sergiou, S., Geraga, M., Phillips, M., McNeill, L.C., Shillington, D.J., Seibert, C., Expedition 381 Participants, 2025. Data report: Age-depth model of the Corinth syn-rift sequence, Site M0079, IODP Expedition 381. In: McNeill, L.C., Shillington, D.J., Carter, G.D.O. (Eds.), Corinth Active Rift Development. Proceedings of the International Ocean Discovery Program, 381: College Station, TX (International Ocean Discovery Program). https://doi.org/10.14379/iodp.proc.381.201.2025.

Pérez-Gussinyé, M., Collier, J.S., Armitage, J.J., et al., 2023. Towards a process-based understanding of rifted continental margins. Nat. Rev. Earth Environ. 4, 166–184. https://doi.org/10.1038/s43017-022-00380-y.

Perissoratis, C., Piper, D.J.W., Lykousis, V., 2000. Alternating marine and lacustrine sedimentation during late Quaternary in the Gulf of Corinth rift basin, central Greece. Mar. Geol. 167 (3–4), 391–411. https://doi.org/10.1016/S0025-3227(00)00038-4.

Peron-Pinvidic, G., Manatschal, G., the IMAGinING RIFTING Workshop Participants, 2019. Rifted margins: state of the art and future challenges. Front. Earth Sci. 7, 218. https://doi.org/10.3389/feart.2019.00218.

Reille, M., De Beaulieu, J.-L., Svobodova, H., Andrieu-Ponel, V., Goeury, C., 2000. Pollen analytical biostratigraphy of the last five climatic cycles from a long continental sequence from the Velay region (Massif Central, France). J. Quat. Sci. 15, 665–685.

Sachpazi, M., Clément, C., Laigle, M., Hirn, A., Roussos, N., 2003. Rift structure, evolution, and earthquakes in the Gulf of Corinth, from reflection seismic images. Earth Planet. Sci. Lett. 216 (3), 243–257. https://doi.org/10.1016/S0012-821X(03)00503-X.

Sadori, L., Koutsodendris, A., Panagiotopoulos, K., Masi, A., Bertini, A., Combourieu-Nebout, N., Francke, A., Kouli, K., Joannin, S., Mercuri, A.M., Peyron, O., 2016. Pollen-based paleoenvironmental and paleoclimatic change at Lake Ohrid (south-eastern Europe) during the past 500 ka. Biogeosciences 13 (5), 1423–1437.

Sánchez Goñi, M.F., Eynaud, F., Turon, J.L., Shackleton, N.J., 1999. High resolution palynological record off the Iberian margin: Direct land-sea correlation for the Last Interglacial complex. Earth Planet. Sci. Lett. 171, 123–137.

Scholz, C.A., Moore Jr., T.C., Hutchinson, D.R., Golmshtok, A.J., Klitgord, K.D., Kurotchkin, A.G., 1998. Comparative sequence stratigraphy of low-latitude versus high-latitude lacustrine rift basins: seismic data examples from the East African and Baikal rifts. Palaeogeogr. Palaeoclimatol. Palaeoecol. 140, 401–420.

Scholz, C.A., Johnson, T.C., Cohen, A.S., King, J.W., Peck, J.A., Overpeck, J.T., Talbot, M. R., Brown, E.T., Kalindekafe, L., Amoako, P.Y.O., Lyons, R.P., Shanahan, T.M., Castañeda, I.S., Heil, C.W., Forman, S.L., McHargue, L.R., Beuning, K.R., Gomez, J., Pierson, J., 2007. East African megadroughts between 135 and 75 thousand years ago and bearing on early-modern human origins. PNAS 104 (42), 16416–16421.

Scholz, C.A., Shillington, D.J., Wright, L.J.M., Accardo, N., Gaherty, J.B., Chindandali, P., 2020. Intrarift fault fabric, segmentation, and basin evolution of the Lake Malawi (Nyasa) Rift. East Africa. Geosphere 16 (5), 1293–1311. https://doi.org/10.1130/ges02228.1.

Sergiou, S., Geraga, M., Pechlivanidou, S., Gawthorpe, R.L., Ninnemann, U., Meckler, A.-N., Modestou, S., Angelopoulou, D., Antoniou, D., Diz, P., McNeill, L., Shillington, D. J., Papatheodorou, G., 2024. Stratigraphic and paleoceanographic alternations within a Mediterranean semi-enclosed, syn-rift basin during Marine Isotope Stage 5: the Gulf of Corinth, Greece. Mar. Geol. 474, 107340. https://doi.org/10.1016/j.margeo.2024.107340.

Shillington, D.J., Scholz, C.A., Chindandali, P.R.N., Gaherty, J.B., Accardo, N.J., Onyango, E., Ebinger, C.J., Nyblade, A.A., Kamihanda, G., Ferdinand, R.W., 2020. Controls on rift faulting in the North Basin of the Malawi (Nyasa) Rift, East Africa. Tectonics 39. https://doi.org/10.1029/2019TC005633 e2019TC005633.

Spratt, R.M., Lisiecki, L.E., 2016. A Late Pleistocene sea level stack. Clim. Past 12, 1079–1092.

Taylor, S.K., Bull, J.M., Lamarche, G., Barnes, P.M., 2004. Normal fault growth and linkage in the Whakatane Graben, New Zealand, during the last 1.3 Myr. J. Geophys. Res. 109, B02408. https://doi.org/10.1029/2003JB002412.

Taylor, B., Weiss, J.R., Goodliffe, A.M., Sachpazi, M., Laigle, M., Hirn, A., 2011. The structures, stratigraphy and evolution of the Gulf of Corinth rift, Greece. Geophys. J. Intl. 185, 1189–1219. https://doi.org/10.1111/j.1365-1246X.2011.05014.x.

Tsoni, M., Iliopoulos, G., Valavani, D., Liapi, E., Papadopoulou, P., Stamoulis, K., Koukouvelas, I., Kontopoulos, N., 2021. Palaeoenvironmental inferences on the Pleistocene deposits of the Charadros River (Rio graben, Western Corinth Gulf, Greece). Quat. Int. 589, 39–54. https://doi.org/10.1016/j.quaint.2021.03.036.

Tzedakis, P.C., Andrieu, V., De Beaulieu, J.L., Crowhurst, S., Follieri, M., Hooghiemstra, H., Magri, D., Reille, M., Sadori, L., Shackleton, N.J., et al., 1997. Comparison of terrestrial and marine records of changing climate of the last 500,000 years. Earth Planet. Sci. Lett. 150, 171–176.

Tzedakis, P., Hooghiemstra, H., Palike, H., 2006. The last 1.35 million years at Tenaghi Philippon: revised chronostratigraphy and long-term vegetation trends. Quat. Sci. Rev. 25, 3416–3430.

Van Avendonk, H.J.A., Lavier, L., Shillington, D.J., Manatschal, G., 2009. Extension of continental crust at the margin of the eastern Grand Banks, Newfoundland. Tectonophysics 468 (1–4), 131–148. https://doi.org/10.1016/j.tecto.2008.1005.1030.

Walsh, J.J., Childs, C., Imber, J., Manzocchi, T., Watterson, J., Nell, P.A.R., 2003. Strain localisation and population changes during fault system growth within the Inner Moray Firth, Northern North Sea. J. Struct. Geol. 25, 307–315. https://doi.org/10.1016/S0191-8141(02)00028-7.

Watkins, S.E., Whittaker, A.C., Bell, R.E., Brooke, S.A.S., Ganti, V., Gawthorpe, R.L., McNeill, L.C., Nixon, C.W., 2020. Straight from the source's mouth: controls on field constrained sediment export across the entire active Corinth rift, central Greece. Basin Res. 32, 1600–1625. https://doi.org/10.1111/bre.12444.

Webber, S., Norton, K.P., Little, T.A., Wallace, L.M., Ellis, S., 2018. How fast can low-angle normal faults slip? Insights from cosmogenic exposure dating of the active Mai'iu fault, Papua New Guinea. Geology 46, 227–230. https://doi.org/10.1130/G39736.1.

Wedmore, L.N.J., Biggs, J., Williams, J.N., Fagereng, Å., Dulanya, Z., Mphepo, F., Mdala, H., 2020. Active Fault Scarps in Southern Malawi and Their Implications for the Distribution of Strain in Incipient Continental Rifts. Tectonics 39 (3). https://doi.org/10.1029/2019TC005834 e2019TC005834.

Withjack, M.O., Schlische, R.W., Olsen, P.E., Kinney, S.T., 2024. Chapter 3 - The rifted margin of eastern North America: insights into rifting, igneous activity, and breakup. In: Chiarella, D., Scarselli, N., Adam, J. (Eds.), Regional Geology and Tectonics, Second edition. Elsevier, pp. 53–83. https://doi.org/10.1016/B978-0-444-64136-6.00001–4.

Wright, L.J.M., Scholz, C.A., Muirhead, J.D., Shillington, D.J., 2023. Heterogeneous strain distribution in the Malawi (Nyasa) Rift, East Africa: Implications for rifting in magma-poor, multi-segment rift systems. Tectonics 42. https://doi.org/10.1029/2022TC007486 e2022TC007486.

Zwaan, F., Alves, T.M., Cadenas, P., Gouiza, M., Phethean, J.J.J., Brune, S., Glerum, A.C., 2024. (D)rifting in the 21st century: key processes, natural hazards, and geo-resources. Solid Earth 15, 1028–9890. https://doi.org/10.5194/se-15-989-2024.